Impaired phagocytosis directs human monocyte activation in response to fungal derived β-glucan particles

Giorgio Camilli, Elif Eren, David Williams, Vishukumar Aimanianda, Etienne Meunier, Jessica Quintin

Impaired phagocytosis directs human monocyte activation in response to fungal derived β-glucan particles

Giorgio Camilli[1], Elif Eren[2], David L. Williams[3], Vishukumar Aimanianda[4], Etienne Meunier[2], and Jessica Quintin[1#]

[1] Immunology of Fungal Infections, Department of Mycology, Institut Pasteur, Paris, France.
[2] Institut de Pharmacologie et Biologie Structurale, IPBS, Université de Toulouse, CNRS, UPS, Toulouse, France.
[3] Department of Surgery, Center of Excellence in Inflammation, Infectious Disease and Immunity, James H. Quillen College of Medicine, East Tennessee State University, Johnson City, Tennessee, USA.
[4] Unité des Aspergillus Department of Mycology, Institut Pasteur, Paris, France.

Keywords: Monocytes, phagocytosis, fungi, β-glucan, inflammation

[#] ***Corresponding author :***
Dr. Jessica Quintin
Immunology of Fungal Infections
Mycology Department
Bâtiment Metchnikoff (67)
Institut Pasteur
25, rue du Docteur Roux
75015 Paris, France
Tel: +33 (0)1 44 38 94 54
Fax: +33 (0)1 40 61 31 15
Mail: jessica.quintin@pasteur.fr

Abbreviations
AI : Alkali Insoluble
AS : Alkali Soluble
ASC : Apoptosis-associated Speck-like Protein Containing a CARD
CARD : Caspase recruitment domain
CD : Cluster of differentiation
CR : Complement receptor
Cyt D : Cytochalasin D
DCs : Dendritic cells
DPI : Diphenyleneiodonium
GAPDH : Glyceraldehyde-3-phosphate dehydrogenase
HK : heat-killed
HK-C.a. : heat-killed *Candida albicans*
IκBα : Inhibitor of NF-κB, alpha
IL: Interleukin
ITAM : Immunoreceptor tyrosine-based Activation Motif
LPS : Lipopolysaccharide
MALT : Mucosa-associated lymphoid tissue lymphoma translocation protein
NADPH : Nicotinamide adenine dinucleotide phosphate hydrate
NF-κB : nuclear factor kappa-light-chain-enhancer of activated B cells
NLRP3: NACHT, LRR and PYD domains-containing proteins 3

PBMC : Peripheral blood mononuclear cell
PI3K : Phosphatidylinositol 3-kinase
PRR : Pattern recognition receptor
ROS : Reactive oxygen species
SHIP : SH2-containing inositol phosphatase
Syk : Spleen tyrosine kinase
TLR : Toll-like receptor
TNFα : Tumor necrosis factor alpha α

Abstract

Recognition of the fungal cell wall carbohydrate β-glucan by the host receptor Dectin-1 elicits broad immunomodulatory responses, such as phagocytosis and activation of oxidative burst. These responses are essential for engulfing and killing fungal pathogens. Phagocytic monocytes are key mediators of these early host inflammatory responses to infection. Remarkably, whether phagocytosis of fungal β-glucan leads to an inflammatory response in human monocytes remains to be established. Here, we show that phagocytosis of heat-killed *Candida albicans* is essential to trigger inflammation and cytokine release. By contrast, inhibition of actin-dependent phagocytosis of particulate (1-3,1-6)-β-glucan induces a strong inflammatory signature. Sustained monocyte activation, induced by fungal β-glucan particles upon actin cytoskeleton disruption, relies on Dectin-1 and results in the classical caspase-1 inflammasome formation through NLRP3, generation of an oxidative burst, NF-κB activation, and increased inflammatory cytokine release. PI3K and NADPH oxidase were crucial for both cytokine secretion and ROS generation, whereas Syk signaling mediated only cytokine production. Our results highlight the mechanism by which phagocytosis tightly controls the activation of phagocytes by fungal pathogens and strongly suggest that actin cytoskeleton dynamics are an essential determinant of the host's susceptibility or resistance to invasive fungal infections.

Introduction

Prior to the mid-1990s, innate immunity was considered to only be required to 'ingest and kill' microorganisms during the course of an infection, providing the host with time to trigger an effective and specific adaptive immune response. However, the discovery of Toll-like receptors led to a revolution in our understanding of the specific role of innate immunity and how the host immune system is activated upon microbial recognition. Several major classes of pathogen-recognition receptors (PRR) have now been described, each with specificity for conserved pathogen structures [1]. A single fungal species, such as *Candida albicans*, is recognized by multiple PRR, including Toll-like receptor (TLR)1, TLR2, TLR4, TLR6, TLR9, mannose receptor (MR), Dectin-1, Dectin-2, galectin-3, and the lectin domain of complement receptor 3 (CR3) (reviewed in [2]).

Recognition of the most abundant fungal cell wall polysaccharide, β-glucan, by Dectin-1 plays an essential role in the host response to fungal infection [3, 4]. Dectin-1 signaling activates antimicrobial innate immune responses, including phagocytosis and the production of reactive oxygen species (ROS) in myeloid cells [5, 6]. Interestingly, Dectin-1 activation requires a phagocytic synapse, mediated by the binding of particulate glucans, and not by small soluble β-glucan molecules [7]. This synapse allows the phosphorylation of the hemITAM (hemi-immunoreceptor tyrosine-based activation motif) by excluding regulatory phosphatases [7]. Notably, however, the use of either yeast or β-glucan with low purity in a majority of the studies has contributed to conflicting conclusions regarding the role of β-glucan in inducing an inflammatory cytokine response. For example, it has been reported that zymosan, a β-glucan-enriched crude preparation of the *Saccharomyces cerevisiae* fungal cell wall, potentiate cytokine secretion via TLR2 and Dectin-1 signaling [8]. By contrast,

microglial cells, RAW cells (a macrophage cell line) or thioglycollate-elicited macrophages fail to secrete cytokines following exposure to pure particulate β-glucan [9, 10]. Walachowski and colleagues reported that enriching the cell wall fraction of β-glucan from 15% to 75% removes TLR ligands while preserving Dectin-1 activity in murine macrophages [11]. Furthermore, the most enriched extracts trigger very low nuclear factor kappa-light-chain-enhancer of activated B cells (NF-κB) activity and cytokine production [11].

The majority of these studies investigating the mechanisms of enriched or pure fungal β-glucan-induced inflammatory cytokine response rely upon mouse macrophages and dendritic cells (DCs). Strikingly, variation in the reported role of β-glucan in triggering inflammation also relies on cell programming. For example, using pure β-glucan particles, depleted zymosan, or curdlan, several studies describe that GM-CSF treated mouse macrophages and dendritic cells, but not M-CSF treated macrophages, produce cytokines in response to glucan stimulation [12-14]. Pure glucan activation of mouse DCs is Dectin-1 and spleen tyrosine kinase (Syk) dependent [15, 16] and is terminated by internalization of Dectin-1. Thus, the blockade of phagocytosis permits continued receptor signaling at the cell surface [13, 14]. Hence, despite numerous reports highlighting β-glucan as a key molecule for host phagocytic cell activation, crucial information regarding the specific response of human mononuclear phagocytes to this molecule is still lacking.

Monocytes have long been considered as developmental intermediates between bone marrow progenitors and differentiated tissue macrophages. However, some DCs and tissue macrophages do not originate from monocytes in non-inflammatory and homeostatic conditions. [17, 18]. Furthermore, monocytes perform specific inflammatory functions during infection, such as producing inflammatory mediators, tumor necrosis factor α (TNFα), nitric

oxide and reactive oxygen species [17, 18] and represent key mediators of early host responses to microbes, including fungi [19]. Moreover, the generation of innate immune memory upon challenge with fungal molecules (i.e. β-glucan) highlights the important role of monocytes in regulation of the host responses to infections and has also gained attention for its potential therapeutic implications [20, 21].

Here, we performed a systematic investigation of the role of phagocytosis on fungal β-glucan-induced inflammation in human monocytes. Our results demonstrate that actin cytoskeleton disruption induced inflammatory cytokine release and enhanced ROS production upon stimulation with a branched *C. albicans* (1-3)-β-glucan. We demonstrate that the synergistic effect on cytokine secretion and ROS generation observed during actin disruption and β-glucan stimulation was dependent upon Dectin-1, phosphatidylinositol 3-kinase (PI3K), and nicotinamide adenine dinucleotide phosphate hydrate (NADPH) oxidase. Conversely, the role of Syk signaling was limited to cytokine production. We further found that the NACHT, LRR, and PYD domains-containing proteins 3 (NLRP3) inflammasome senses phagocytosis inhibition-associated β-glucan–mediated activation to induce caspase-1 cleavage and interleukin (IL)1β release in human monocytes. These findings highlights the specific mechanism by which phagocytosis tightly controls the activation of primary human monocytes and suggest that actin cytoskeleton dynamics may drive host's susceptibility or resistance to invasive fungal infections.

Results

Phagocytosis and actin dynamics differently impact monocyte responses to *C. albicans* and β-glucans P

Initially, we hypothesized that engulfment of fungal pathogens by human phagocytes is not only a killing and scavenging process but also a potent mechanism of inflammation regulation. To test this hypothesis, we assessed the role of phagocytosis in the immune response triggered by monocytes upon encounter with heat-inactivated/killed (HK) *Candida albicans*. We used HK *C. albicans* to avoid any active delay in the phagocytic process triggered by live and virulent *C. albicans* [22]. Following exposure of primary human monocytes isolated from blood of healthy donors, we observed that HK *C. albicans* induced the release of TNFα, IL6, IL1β, and IL10 (Figure 1A). This inflammatory response was abrogated when phagocytosis was impaired by the actin polymerization inhibitor, cytochalasin D (CytD)(Figure 1A and SI Figure 1). The inflammatory response was also induced following exposure to HK *Saccharomyces cerevisiae* and inhibited when phagocytosis was blocked (Figure 1B).

The cell wall of yeast, such as *C. albicans* and *S. cerevisiae,* is composed of two main layers [23]. The outer layer is highly enriched with *O*- and *N*-linked glyco/mannoproteins whereas the inner layer contains the skeletal polysaccharides chitin and branched-β-1-3 glucan that confer strength and cell shape. The outer cell wall layer is attached to this framework predominantly by glycosylphosphatidylinositol (GPI)-remnants that are linked to the skeleton through a more flexible β-1-6 glucan [23]. Alkali treatment of the yeast allows separation of the different cell wall carbohydrates. No inflammatory cytokine release was observed following stimulation of human monocytes with the alkali soluble (AS) fraction of *S.*

cerevisiae, containing mannoproteins and β-(1-6)-glucan, regardless of the presence or absence of CytD (Figure 1C). Incubation of monocytes with the Alkali Insoluble (AI) fraction containing branched β-(1-3)-glucan, chitin and β-(1-6)-glucan neither did trigger an inflammatory response. Interestingly however, impairing phagocytosis before stimulation with the AI fraction led to strong cytokine release in the supernatant (Figure 1C). Within this fraction, we observed that branched β-(1-3)-glucan (associated with less than 5% chitin) was mimicking the AI fraction whereas β-(1-6)-glucan alone (from AS fraction) were not able to replicate the inflammatory effect observed with Cyt D (Figure 1C). To determine the structure required to trigger the release of cytokine by monocytes when phagocytosis is blocked, we used pure insoluble branched β-(1-3)-glucan from *S. cerevisiae* and *C. albicans*. Both branched β-(1-3)-glucans induced monocyte activation when their engulfment was impaired by Cyt D treatment in a dose dependent manner (Figure 1D; SI Figure 1). The increase in cytokine release was more potent at lower concentrations with branched *C. albicans* β-(1-3)-glucan (Figure 1D). As previously reported for mouse DCs and macrophages [12, 13, 15, 16], we observed that large curdlan particles (insoluble linear β-(1-3)-glucan) stimulated human monocytes in an actin-dependent manner, but laminarin (soluble branched β-(1-3,1-6)-glucan)) did not activate monocytes, even when phagocytosis was inhibited (Figure 1E). To rule out potential aggregations interference (SI Figure 2), mild sonication of branched *C. albicans* β-(1-3)-glucan was performed which had no effect on monocyte activation triggered in presence of Cyt D (Figure 1F). Increasing the concentration of branched *C. albicans* β-(1-3)-glucan, or of AI fraction together with Cyt D, showed similarly increased cytokine expression (Figure 1G). By contrast, increasing the concentration of the AS fraction did not induce cytokine expression even in the presence of Cyt D. Of note, combining the AS fraction and the AI fraction had no inhibitory effect on the release of cytokines mediated by AI (Figure 1G). Similarly, increasing the concentration of HK *C. albicans* augmented the initial

inflammatory response, but blocking phagocytosis still inhibited the release of cytokines. As actin polymerization inhibiton led to an increase in cytokine expression which we confirmed by using latrunculin B (Figure 1H), we next wanted to test the impact of an actin filament polymerizing and stabilizing drug. We observed that jasplakinolide had no effect on HK *C. albicans*-mediated inflammation or on the absence of response with *C. albicans*-branched β-(1-3)-glucan (Figure 1H). Finally, whereas blocking actin polymerization (Cyt D or Lantrunculin B), clathrin-mediated endocytosis using chlorpromazine, or acidification of the phagolysosome with chloroquine inhibited cytokine production upon HK *C. albicans* stimulation, only the inhibition of actin polymerization (Cyt D or Lantrunculin B) was able to activate the release of cytokines by human monocytes incubated with *C. albicans* β-(1-3)-glucan (Figure 1H).

IL-1β release is mediated by the canonical NLRP3 inflammasome in phagocytosis-impaired monocytes I

As impaired phagocytosis triggered the secretion of IL1β by human monocytes upon branched *C. albicans* β-(1-3)-glucan exposure, we wanted to determine how IL1β is activated. The bioactivity of IL1β is controlled by activation of the inflammasome [24]. The inactive precursor molecule, pro-IL1β, must be converted to the mature form to become functional [24]. Processing of pro-IL1β is mediated by the enzyme caspase-1, which is activated by multi-protein inflammasome complexes such as NLRP3. In macrophages and DCs, activation of the NLRP3 inflammasome requires two separate signals [24]. However, in human monocytes, lipopolysaccharide (LPS) from Gram-negative bacteria is sufficient to trigger caspase-1-dependent IL1β maturation and secretion [25]. This activity in monocytes is clearly distinct from the two-step activation observed in macrophages and DCs [26]. As such, it has

become evident that in monocytes LPS is directly sensed by caspase-11 or its human orthologs caspase-4 and caspase-5 in the cytosol to trigger cell death or activate the NLRP3 inflammasome [27, 28]. In addition, human caspase-4 and caspase-5 regulate the one-step non-canonical inflammasome activation in human monocytes [29]. Finally in human monocytes, extracellular LPS triggers an alternative inflammasome that relys upon TLR4 - TRIF - RIPK1 - (FADD) – caspase-8 signaling upstream of NLRP3-ASC-caspase-1 [25]. Interestingly, both caspase-1 and -8 are associated with linear- β-glucan/Dectin-1 signaling in human DC [30, 31]. Of note, although not associated with fungi or β-glucan, the one-step non-canonical inflammasome activation by LPS is Syk-dependent, a crucial kinase required for β-glucan/Dectin-1 signaling [29].

Thus, we wanted to determine which of these caspases mediated mature IL1β release following concomitantly phagocytosis inhibition and *C. albicans* β-(1-3)-glucan exposure in human monocytes. We observed that the pan-caspase inhibitor Z-VAD blocked the release of IL1β by phagocytosis-impaired human monocytes upon *C. albicans* β-(1-3)-glucan exposure, suggesting caspases mediate IL1β processing (Figure 2A). Only the caspase-1 inhibitor Z-YVAD, but not caspase-8 Z-IETD nor caspase-4 and -5 Z-LEVD inhibitors inhibited IL1β release (Figure 2A). Thus, when phagocytosis was impaired, IL1β release was mediated by the protease caspase-1 following exposure of human monocyte to *C. albicans* β-(1-3)-glucan. Immunoblot experiments confirmed that concomitant Cyt D/β-glucan treatment promoted both caspase-1 activation and IL1β processing and release in monocytes (Figure 2B), thus confirming the involvement of an inflammasome in this process. A feature of the canonical inflammasome is its ability to induce ASC polymerization for efficient IL1β processing after receptor activation [24]. This structure is called a speck and can be imaged by fluorescence [32]. Impairing actin polymerization prior to *C. albicans*-branched β-(1-3)-glucan exposure

strongly activated the formation of ASC specks, a phenomenon only mildly induced when actin polymerization was intact (Figure 2C and D). The NLRP3 inflammasome promotes both caspase-1 and -8-mediated IL1β processing and release in response to β-glucans and fungi [33]. To determine whether NLRP3 could be the mediator of Cyt D/β-glucan-induced IL1β processing and release, we used the potassium channel inhibitor glibenclamide, observing that a potassium signal was required for β-glucan-triggered IL1β release (Figure 2E). Similar results were obtained when using MCC950, a specific NLRP3 inhibitor, in which IL1β release was strongly diminished (Figure 2E). Intriguingly, although the caspase recruitment domain (CARD)9 - Mucosa-associated lymphoid tissue lymphoma translocation protein (MALT)1 pathway promotes pro-inflammatory cytokine transcription [34] , the paracaspase MALT1 inhibitor did not significantly alter mature IL1β release from human monocytes stimulated with Cyt D/β-glucan (Figure 2E).

Dectin-1, Syk, and PI3K pathways control β-glucan signaling in human phagocytosis-impaired monocytes D

Signalling of β-glucan is mediated by a limited number of surface PRRs on mononuclear phagocytes [35]. As cytokine release by human monocytes, inhibited for phagocytosis, was observed following exposure to *C. albicans* β-(1-3)-glucan we therefore investigated which receptors and signaling pathways were involved.

Following antibody-mediated inhibition of TLR2 or CR3 receptors, we observed no effect on the release of cytokines whereas blockade of Dectin-1 completely inhibited cytokine secretion mediated by monocytes whose phagocytosis is impaired and stimulated with *C. albicans* β-(1-3)-glucan (Figure 3A). In addition, only a partial inhibition of IL6 cytokine release was observed using a combination of antibodies against CD11b and CD18 subunits of CR3,

described as more effective in comparison with blocking the CD11b chain alone [36] (SI Figure 3).

Dectin-1 activates cellular responses via the Syk/CARD9 [37]. Inhibiting Syk kinase in our human primary monocytes system diminished the amount of cytokines produced upon stimulation with *C. albicans*-branched β-(1-3)-glucan, suggesting that the stimulation of phagocytosis-impaired monocytes by Dectin-1 is Syk kinase-dependent (Figure 3B). Phosphoinositide-3 kinase (PI3K) is also a downstream mediator of the Dectin-1 signaling pathway [38]. Interestingly, inactivation of PI3K, using wortmannin, had a strong inhibitory effect on cytokine production of β-(1-3)-glucan/Cyt D treated monocytes, suggesting that PI3K is not only working downstream of Syk but in a concomitant pathway as well (Figure 3C).

We next assessed the activation of the crucial transcription factor NF-κB by β-(1-3)-glucan exposure of human monocytes impaired for phagocytosis. Impairing actin polymerization prior to *C. albicans* β-(1-3)-glucan exposure strongly induced phosphorylation of the inhibitor of NF-κB alpha (IκBα) protein (Figure 4A, B). Phosphorylation was less evident when actin polymerization was intact in monocytes treated with by *C. albicans*-branched β-(1-3)-glucan (Figure 4A, B). Of interest, the strong phosphorylation of IκBα observed in monocytes treated with CytD and stimulated by *C. albicans* β-(1-3)-glucan correlated with the degradation of the protein (Figure 4A, B). Finally, both phosphorylation and degradation of IκBα correlated with the activation and translocation of the canonical NF- κB transcription factor into the nuclei (Figure 4C).

Differential role of Syk and PI3K in the inflammatory response triggered by β-glucans in monocytes

The immune response mediated by mononuclear phagocytes upon fungal recognition and engulfment is not solely restricted to induction of inflammatory cytokines. Indeed, pattern-recognition receptors in innate immunity trigger reactive oxygen (ROS) species for intracellular killing of fungi [39]. Therefore, we assessed the production of ROS in our monocytes. Stimulation of monocytes with *C. albicans* β-(1-3)-glucan triggered ROS production compared to the basal level detected in resting cells (Figure 5A, D: vehicle). Similar ROS induction was observed when actin polymerization was blocked in untreated monocytes (Figure 5A, D). However, a strong and synergistic induction of ROS was observed when phagocytosis-impaired monocytes were stimulated with *C. albicans* β-(1-3)-glucan. This induction was NADPH dependent as pharmacological inhibition of oxidase activation with either diphenyleneiodonium (DPI) (Figure 5A) or apocynin (SI Figure 4) reduced the production of ROS in a dose-dependent manner. Inhibition of oxidase activation also reduced the secretion of TNFα, IL6, and IL1β by phagocytosis-impaired monocytes stimulated with *C. albicans* β-(1-3)-glucan (Figure 5B and SI Figure 4).

These results suggest that NADPH-induced ROS are important mediators of the unique inflammatory cytokine signature of phagocytosis-impaired monocytes stimulated with *C. albicans*-branched β-(1-3)-glucan. We, therefore, investigated whether the signaling pathway leading to ROS production shares common mediators with the regulation of cytokine production. ROS generation was observed in monocytes in response to *C. albicans* β-(1-3)-glucan and was blocked by inhibiting either Dectin-1, Syk, or PI3K (Figure 5C, D: DMSO treated). By contrast, inhibition of either Dectin-1 or PI3K, but not Syk, abolished the potent

synergistic ROS release observed in phagocytosis-impaired monocytes stimulated with *C. albicans* β-(1-3)-glucan (Figure 5C, D: Cyt D). This result was surprising given that, unlike the concomittent regulation of cytokine release, we observed that oxidative burst, triggered by a fungal encounter, depended on PI3K and not Syk.

As we observed that inflammatory cytokine release in phagocytosis-impaired monocytes stimulated with *C. albicans* β-(1-3)-glucan was Syk-dependent (Figure 3B), we tested Syk involvement in inflammasome and NF-κB activation. Inhibition of Syk abolished the nuclear translocation of NF-κB transcription factor in phagocytosis-impaired monocytes stimulated with *C. albicans* β-(1-3)-glucan (Figure 6A, B). Similarly, inhibition of Syk activity strongly reduced caspase-1 activation and the release of active IL-1β and caspase-1 in the supernatant (Figure 6C). Therefore, Syk activity is required for inflammasome and NF-κB activation, and cytokine release.

Discussion

The surveillance and elimination of fungal pathogens relies heavily on the sentinel behavior of phagocytic cells of the innate immune system. As such, innate mononuclear phagocytes must recognize, uptake, and kill fungal pathogens. Herein, we demonstrate that phagocytosis of fungal cells or fungal cell wall componenets by human primary monocytes also regulates the inflammatory responses mediated by the host. We demonstrated that the inflammatory HK *C. albicans*-dependent response of monocytes requires phagocytosis and engulfment of the yeast. By contrast, ingestion of insoluble branched *C. albicans* β-(1-3)-glucan is inert and cytokine secretion from human monocytes is induced only when β-(1-3)-glucan remains in the extracellular space. Activation of phagocytosis-impaired-human monocytes by branched

C. albicans β-(1-3)-glucan through Dectin-1 , Syk and PI3K results in cytokines release and NF-κB activation. In addition we observed NLRP3/ASC/caspase-1 inflammasome formation, leading to IL-1β processing and release. Interestingly our results highlight that the increased β-glucan-induced oxidative burst in phagocytosis-impaired monocytes depends on Dectin1 and PI3K but is independent of the canonical Syk pathway.

Blocking actin polymerization, hence phagocytosis, converts *C. albicans*-branched β-(1-3)-glucan into a potent activator of innate responses via the Dectin-1 pathway. This observation is reminiscent of the work of Hernanz-Falcón and colleagues in which the blockade of glucan particles internalization trigger the response of dendritic cells and more specifically mitogen-activated protein kinase (MAPK) activation [13]. One might therefore question the role of phosphatase in the regulation mediated by actin polymerization. One possible candidate could be SH-2 containing inositol 5' polyphosphatase 1 (SHIP1) that has recently been demonstrated to interact with the Dectin-1 hemITAM and selectively modulates reactive oxygen species production in dendritic cells in response to *C. albicans* [40]. However, the study of Blanco-Menéndez and colleagues showed no effect of the SH-2 containing inositol 5' polyphosphatase 1 (SHIP1) on the regulation of the secreted cytokines, which was a hallmark of our study.

Our observation that the insoluble and linear β-glucan curdlan is able to stimulate the release of cytokines from human primary monocytes, in an actin-dependent mechanism is consistent with other studies in murine macrophages and dendritic cells [13-16]. Indeed, the release of cytokines is inhibited when phagocytosis is impaired, a phenomenon reminiscent of what we observed with HK *C. albicans.* However, whereas *C. albicans* yeast are evenly distributed among the monocytes population and phagocytosed in control situation when actin

polymerization is functional, (SI Figure 1), very large curdlan aggregates are sporadically distributed and never phagocytosed (SI Figure 1). Indeed, even if monocytes migrate towards the curdlan aggregate, they only surround and bind the β-(1-3)-glucan curdlan particles without phagocytosis (SI Figure 1 and 24 hours time point, data not shown). However, when actin polymerization is blocked, migration of monocyte is constrained and recognition of β-(1-3)-glucan by Dectin-1 is inhibited. This lack of dectin-1 engagement with β-glucans, reported as well by Hernanz-Falcon et *al.* and Rosas et *al.* in mice [13, 14], is the likely explanation for the impeded cytokine release. Dectin-1 engagement might, however, still occur with HK *C. albicans* or branched β-(1-3)-glucan isolated from *C. albicans* or *S. cerevisiae* as the organisms/particles are more evenly distributed and easily accessible to monocytes (SI Figure 1). Interestingly, whereas Dectin-1 is likely activated by either HK *C. albicans* or branched β-(1-3)-glucan, HK *C. albicans* does not elicit cytokine release when phagocytosis is impaired. This observation is reminiscent of the work of Filler et al., who demonstrated that endothelial cell phagocytosis of live *C. albicans* was necessary for endothelial cell stimulation to occur [41]. Strikingly however, and in contrast with our observation in human monocytes, they also determined that killed *C. albicans* did not induce endothelial cell activation, even though killed *C. albicans* are phagocytozed by endothelial cells [41].

Our data show that impaired uptake of *C. albicans*-branched β-(1-3)-glucan particles results in high release of IL1β associated with NLRP3/ASC/caspase-1 inflammasome formation. This observation suggest that NLRP3 could sense the overstimulation of the Dectin-1 receptor by particulate agonists. Intriguingly, inhibition of the para-Caspase activity of MALT1 did not significantly affect the maturation of IL1β although the CARD9-MALT1 pathway was described to promote pro-inflammatory cytokine transcription. Whether another adaptor from

the Dectin-1 pathway is involved or if MALT1 plays a role independent from its catalytic domains remains to be investigated. However, MALT1 also expresses a Caspase-Activating Recruitment Domain (CARD) essential for the CBM (CARD-BCL-MALT) tripartite complex formation CARD9-BCL10-MALT1 and signal transduction after Dectin-1 engagement. One should not exclude that upon prolonged interactions between these three partners, the (CARD-BCL-MALT) CBM complex could induce a stress detected by the NLRP3 sensor.

The opposite effect on monocyte cytokine responses between whole *Candida albicans* and β-glucan particles is intriguing and raises the question of a putative negative regulation of the phagocytic-dependent cytokine secretion by whole *Candida albicans*. As such, one might hypothesize that mannan in the cell wall of *Candida albicans* acts as a negative regulator of inflammation. Previous studies have shown that mannan contributes to the resistance of *C. albicans* to complement activation and complement component 3 (C3) binding by *C. albicans* [42]. However, adding mannans within the alkali-soluble fraction, to the potent β-glucan inducer in the alkali-insoluble fraction did not inhibit the release of cytokines induced by phagocytosis-impaired monocytes. We can, therefore, exclude that alkali aoluble fractions of yeast contain inhibitors of the β-glucan mediated inflammation. However, alkali-treatment is very stringent, so we cannot yet exclude that surface proteins on *Candida albicans* are responsible for the mirror effect observed.

The discrepancy we observed between the different size of branched β-glucan is also of interest. Such discrepancy in size has already been observed in the signaling mediated by Dectin-1 during which the signal is only transduced when two or more receptors cluster together to form a full ITAM motif. This event only occurs with particulate β-glucans, which cluster the receptor in synapse-like structures from which the regulatory tyrosine

phosphatases CD45 and CD148 are excluded [7]. Similarly, during the submission of this manuscript, Matthew J. Elders and colleagues observed that Dectin-1-mediated immune responses in human dendritic cells is highly dependent on β-glucan particle size and the high production of IL1β. Interestingly blocking internalization allows the production of IL1β [43]. Our present study now suggests that not only the stoichiometry, but also the capacity to be phagocytosed, plays a role in the signaling. Very recently, a study on neutrophils has highlighted the differential reponses obtained when the pathogen encountered is of small size –and phagocytosed-, or of bigger size –hence not phagocytosed [44]. More specifically and elegantly, the study demonstrates that the ability to sense the differential localization of ROS allows neutrophils to adjust the inflammatory response by modulating their own recruitment and cooperation to effectively clear microbes of different size. Whether a similar mechanism is involved in monocytes is still questionable. But such a hypothesis might be supported by the observation that human peripheral blood mononuclear cells (PBMCs) use distinctly Dectin-1 or CR3 receptor and overlapping, but distinct, signaling pathways for the oxidative burst in response to challenge by different physical forms of β-glucan [36].

It is also possible that the source of the cell wall fragment may also be of importance. In this study we focused on the yeast form of *Candida albicans* and its cell wall component β-glucan. But it has been demonstrated that with *Aspergillus fumigatus*, another important human fungal pathogen, in contrast to conidia, hyphal fragments induce NLRP3 inflammasome assembly, caspase-1 activation and IL1β release from a human monocyte cell line [45]. *C. albicans* hyphal β-glucan, but not of yeast, can stimulate the release of IL1β by monocytes-derived-macrophages [46]. The ability of *C. albicans* to switch from a unicellular yeast form into a filamentous hyphal form has been presented as essential for activation of the NLRP3 inflammasome, as *C. albicans* mutants incapable of forming hyphae were defective in

their ability to induce murine macrophage IL1β secretion [47]. By contrast, Mukaremera and colleagues demonstrated that *C. albicans* hyphae stimulate proportionally lower levels of certain cytokines from human PBMCs per unit of cell surface area than yeast cells, but did not suppress cytokine responses when copresented with yeast cells. This latter observation is intriguing as germ tubes with an attached parent yeast cell does not induce a response that would normally be associated with free yeast cells [48].

Our study also raises the question of the importance of phagocytosis in the inflammatory response mediated in situations where phagocytosis is naturally impaired. As such, *Candida albicans* is known to produce potent biofilms rendering it tolerant to antifungal treatment [49]. In such biofilms, innate immune cells can hardly migrate [50] rendering phagocytosis very unlikely. However, soluble matrix β-(1-3)-glucans are accessible [49]. One might hypothesize that the combined detection of non-phagocytosed soluble β-(1-3)-glucans together with the non-phagocytosis of whole *Candida albicans* cells participates in the non-effective immune responses triggered towards *Candida albicans* biofilm.

Materials and methods

Cell isolation

Human PBMCs were separated on Ficoll-Paque (GE Healthcare) by density centrifugation of heparinized blood from healthy donors ("Etablissement Français du Sang" EFS, Paris, France, habilitation HS-2015-25101). Monocytes were purified by negative selection using the Pan Monocyte Isolation Kit (Miltenyi Biotec, Bergisch Gladbach, Germany). The purity evaluated by flow cytometry was routinely >90%. Cells were seeded at $5x10^5$ cells/ml in RPMI 1640, supplemented with 2 mM GlutaMax, 50 μg/ml gentamicin and 1 mM sodium pyruvate (Gibco, Invitrogen, Carlsbad, CA, USA). Cells were maintained in a humidified atmosphere of 5% CO_2 at 37°C.

Stimulation experiments

When indicated $1x10^5$monocytes were pretreated with DMSO (SIGMA), cytochalasin D (1 μg/ml, C8273, SIGMA), latrunculin B (2,5 μM, 428020, EMD Millipore), jasplakinolide (0,1 μM, 420127, EMD Millipore), chlorpromazine (1 μg/ml, C8138, SIGMA) or chloroquine (25 μM, C6628, SIGMA) for 1 hour. Different stimuli were then added to the cells: heat-inactivated *Candida albicans* (UC820 strain, 30 min at 95 degrees, 10^5/ml unless otherwise stated), heat-inactivated *Saccharomyces cerevisiae* (BY471 strain, 30 min at 95 degrees, 10^6/ml unless otherwise stated), purified β–glucan from *Candida albicans* (1 μg/ml unless otherwise stated; depyrogenated was provided by Dr. David L. Williams, East Tennessee State University) (β–glucan from *Candida albicans* was purified as described [46]); purified β–glucan from *Saccharomyces cerevisiae* (1 or 10 μg/ml, G5011, SIGMA); Laminarin from *Laminaria digitata* (1 or 10 μg/ml, L9634, SIGMA); curdlan from *Alcaligenes faecalis* (1 or 10 μg/ml, Wako); alkali-soluble and insoluble fractions from *Saccharomyces cerevisiae* (1, 10

or 50 μg/ml); β-(1-6)-glucan from *Saccharomyces cerevisiae* (1 or 10 μg/ml); β-(1-3)/(1-6)-glucan from *Saccharomyces cerevisiae* (1 or 10 μg/ml). Preparations from the cell wall of *Saccharomyces cerevisiae* (BY4741 strain) were provided by Vishukumar Aimanianda, Institut Pasteur, Paris, France. Alkali-insoluble fractions was prepared and β-(1-6)-glucan was purified from from *S. cerevisiae* (BY4741 strain) as described earlier [51]. To obtain alkali-soluble fraction, in brief, the excess of $NaBH_4$ in the supernatant after NaOH-$NaBH_4$ treatment of the sediment (cell wall fraction; [51]) was destroyed using 2% acetic acid, followed by dialysis against water for until neutrality and freeze drying. The β-(1-3)-glucan (approximately 4% branched by β-(1-6)-linkage; [52]) was purified from alkali-insoluble fraction using the protocol described earlier [53]. The stimuli were pre-incubated for 1h at room temperature with (10μg/ml) polymyxin B (92283, SIGMA).

For inhibition, before adding DMSO or cytochalasin D, monocytes were preincubated for 30 min with: 20 μM Ac-YVAD-cmk (caspase-1 inhibitor, inh-yvad, InvivoGen); 20 μM z-VAD-fmk (pan-caspase inhibitor, G7231, Promega); 20 μM z-IETD-fmk (caspase-8 inhibitor, 1148, BioVision); 10 μM z-LEVD-fmk (caspase-4/5 inhibitor, ALX-260-142, Alexis); 20 μM z-VRPR-fmk (MALT1 inhibitor, ALX-260-166, Alexis); 1 μM MCC950 (NLRP-3 inhibitor, CP-456773, SIGMA); 125 μM glibenclamide (inhibitor of potassium efflux, G0639, SIGMA); 1-2 μM Syk inhibitor (574711, EMD Millipore); 100 nM (wortmannin, tlrl-wtm, InvivoGen); 5 μg/ml anti-Dectin-1 Ab (ab82888, abcam) or 5 μg/ml IgG1 Isotype control (401402, Biolegend); 10 μg/ml anti-TLR2 Ab (16-9922-82, eBioscience) or 10 μg/ml IgG2a Isotype control (16-4724-82, eBioscience); 10 μg/ml anti-CR3 Ab (AF1730, R&D SYSTEM) or 10 μg/ml normal goat IgG control (AB-108-C, R&D SYSTEM); 1-5-10 μM DPI (NADPH oxidase inhibitor, D2926, SIGMA); 0,1 mM Apocynin (NADPH oxidase inhibitor, 178385,

SIGMA). The CR3 receptor was also blocked using a combination of antibodies against both the CD11b and CD18 subunits (SI Figure 3) as previously described [36]: LM2/1, a mouse anti-human IgG1 monoclonal antibody to the I domain of CD11b chain of CR3 (10 μg/mL; eBioscience); VIM12, a mouse monoclonal IgG1 anti-human antibody to the lectin domain of CD11b chain of CR3 (10 μg/mL; invitrogen); and IB4, a mouse monoclonal IgG2a anti-human antibody to the CD18 chain of CR3 (10 μg/mL; Calbiochem). Isotype controls, mouse IgG1 (clone P3; eBioscience) and mouse IgG2a (clone eBM2A; eBioscience) were used at the same concentration as the blocking antibodies. Positive controls for inhibitors that did not show any effect in our sytem are depicted in SI Figure 7.

Cytotoxicity assay

To exclude any impact of cytotoxicity of the different inhibitory coumpounds used in this study we measured lactate dehydrogenase (LDH) activity released from the cytosol of damaged cells into the supernatant (SI Figure 5). LDH release was measured using the Cytotoxicity Detection kit (Roche, Mannheim, Germany) according to the manufacturer's instructions. Monocytes were pretreated with the indicated inhibitors for 30 min (see "Stimulation experiments" for all the concentrations used) and exposed to CytD (1 μg/ml) for 1h. Monocytes were then stimulated with 1 μg/ml β-glucan C.a. for 24h before cell−free culture supernatants were collected and incubated with LDH assay solution at 25˚C for 30 min. The optical density values were analyzed at 490 nm by subtracting the reference value at 620 nm. The experiment was repeated at least three times and the results were expressed as a percentage of the maximum LDH release, obtained by lysing the cells in 1% Triton X‑100.

Immunoblot

Total cellular protein extracts were obtained by lysing $2x10^6$ cells for 30 min at 4°C in lysis buffer (Pierce RIPA Buffer) in the presence of protease and phosphatase inhibitors (ROCHE). Samples were centrifuged for 15 minutes at 4°C, 15000 RPM and supernatants collected in new tubes. Cell culture supernatants were collected and precipitated in Tricloroacetate (TCA) 10% (v/v) for 1 hour on ice. Proteins were centrifuged for 30 min/4°C at 15000 RPM and pellets washed with ice-cold acetone. Samples were centrifuged for 15 min, 4°C, 15000 rpms. Proteins from cell extracts and supernatants were suspended in Laemli Buffer 1X and boiled at 95°C for 10 min. Proteins from cell extracts and supernatants were either mixed using a ratio 1:1 or individually kept. 30µL of each sample were allowed to migrate by SDS-PAGE and transferred with the iBlot apparatus (Life Technologies). Immunoblotting was performed by use of the following primary antibodies: anti-phospho-IKB (5A5), anti-IKB (44D4), anti-NLRP3 (D4D8T), anti-Caspase-1 (D7F10), anti-IL1β (3A6) (all from Cell Signalling). Anti-mouse or anti-rabbit IgG, HRP-linked antibodies (GE Healthcare) were used as secondary antibodies, and protein bands were visualized by use of ECL Prime (GE Healthcare) and a myECL imager (Thermo Fisher Scientific). Proteins were normalized for Glyceraldehyde-3-phosphate dehydrogenase (GAPDH, Santa Cruz Biotechnology) by use of ImageJ software (NIH, Bethesda, MD, USA).

Cytokine assay

TNFα, IL6 and IL1β levels on monocytes were determined by enzyme-linked immunosorbent assays (ELISA) on 24h monocyte cell culture supernatants according to manufacturer's instructions (R&D Systems). For IL10, supernatants from human cell cultures were collected and cytokine detection was performed using the ELISA MAX™ Standard Set (BioLegend), according to the manufacturer's instructions.

Reactive oxygen species measurements

For measurement of reactive oxygen species production, a luminol-enhanced chemiluminescence assay was used. $1x10^5$ monocytes, resuspended in Hank's Balanced Salt Solution (HBSS, GIBCO), were seeded in a white 96-well assay plate (Corning) and pre-treated for 30 min with the vehicle or the inhibitors indicated. Cells were then treated for 1h with DMSO or cytochalasin D diluted in Hank's Balanced Salt Solution (HBSS). The β-glucan (1 μg/ml) and Luminol (50 μM) were added, and light emission was measured every 2 min for a period of 120 min using the Synergy H1 microplate reader (Biotek). The light emission levels are expressed as RLU (Relative Light Units = luminescence given by the luminometer). All measurements were performed at least in duplicate, depending on the number of cells available.

Fluorescence

Treated monocytes were fixed in 4% formaldehyde solution for 10 min at 37°C, then washed with phosphate buffered saline (PBS) and excess of formaldehyde solution was quenched for 10 min with 0.1M of Glycine. Cells were permeabilized with Saponin 0.2%/BSA 3% for 20 min at 4°C. Antibodies against p65 (1/800, L8F6, Cell Signalling), ASC (1/500, sc-22514-R, clone N.15, SantaCruz Biotechnologies) are incubated at 4°C in Saponin/BSA solution overnight. The day after, samples were incubated with secondary antibodies anti-mouse-488 and anti-rabbit-568 (Invitrogen). Hoescht (Invitrogen) is used at 1/5000 for nucleus staining. Coverslips were mounted using Vectashield mounting medium (Vectorlabs) and sealed. Cells were imaged using a spinning disk microscope with a 60X oil objective. Images are analyzed using Image J software.

Internalization assay

HK *C. albicans* were labeled with fluorescein isothiocyanate (FITC; SIGMA) for 1h in the dark and thoroughly washed with phosphate buffered saline (PBS) before incubating with the effectors. For β-glucan-FITC labelling, in brief, glucan preparations were suspended in FITC solution prepared in carbonate buffer (pH 9.6) (glucan:FITC concentration ratio of 5:1), incubated overnight at 4°C, washed with carbonate buffer (3x), with PBS (1x) and then suspended in PBS. Monocytes were then incubated with HK fungi or β-glucan for 2h. For quenching of not internalized fluorescein isothiocyanate (FITC)-particles, cells were treated for 3 min with trypan blue (0.2%; Molecular Probes, Life Technologies). Internalization was assessed with an EVOS FL Cell Imaging system (Thermo Fisher Scientific).

Statistics

In vitro monocyte experiments were performed at least 3 times, and the results were analyzed using a Wilcoxon matched-pairs signed-rank test (unless otherwise stated). Synergy was defined when ROS level produced upon the concomitant Cyt D and β-glucan treatment was significantly greater than the addition of ROS levels produced with Cyt D and β-glucan alone. A P value below 0.05 was considered statistically significant. All data were analyzed using GraphPad Prism software version 5.0 (La Jolla, CA, USA). Data are shown as means ± standard errors of the means.

Acknowledgments

We thank Dr Molly Ingersoll for critical reading of the manuscript. We thank Rachel Lavenir for her technical help thorough the study. G.C. and J.Q. were supported by the Institut Carnot Pasteur MI grant ANR 11-CARN 017-01 and the ANR JCJC grant ANR-16-CE15-0014-01 (to J.Q.). E.E. and E.M. were supported by the FRM « Amorçage Jeunes Equipes » grant

AJE20151034460 and ATIP-Avenir Grant (to E.M.). This work was also supported, in part, by National Institutes of Health grants GM119197, GM53522 and GM083016 to D.L.W.

Conflict of Interest

The authors declare no fincancial or commercial conflict of interest

References

[1] **Akira, S., Uematsu, S. and Takeuchi, O.,** Pathogen recognition and innate immunity. *Cell* 2006. **124**: 783-801.

[2] **Gow, N. A., Netea, M. G., Munro, C. A., Ferwerda, G., Bates, S., Mora-Montes, H. M., Walker, L.et al.,** Immune recognition of Candida albicans beta-glucan by dectin-1. *J Infect Dis* 2007. **196**: 1565-1571.

[3] **Taylor, P. R., Tsoni, S. V., Willment, J. A., Dennehy, K. M., Rosas, M., Findon, H., Haynes, K.et al.,** Dectin-1 is required for beta-glucan recognition and control of fungal infection. *Nat Immunol* 2007. **8**: 31-38.

[4] **Gantner, B. N., Simmons, R. M. and Underhill, D. M.,** Dectin-1 mediates macrophage recognition of Candida albicans yeast but not filaments. *Embo J* 2005. **24**: 1277-1286.

[5] **Herre, J., Marshall, A. S., Caron, E., Edwards, A. D., Williams, D. L., Schweighoffer, E., Tybulewicz, V.et al.,** Dectin-1 uses novel mechanisms for yeast phagocytosis in macrophages. *Blood* 2004. **104**: 4038-4045.

[6] **Underhill, D. M., Rossnagle, E., Lowell, C. A. and Simmons, R. M.,** Dectin-1 activates Syk tyrosine kinase in a dynamic subset of macrophages for reactive oxygen production. *Blood* 2005. **106**: 2543-2550.

[7] **Goodridge, H. S., Reyes, C. N., Becker, C. A., Katsumoto, T. R., Ma, J., Wolf, A. J., Bose, N.et al.,** Activation of the innate immune receptor Dectin-1 upon formation of a 'phagocytic synapse'. *Nature* 2011. **472**: 471-475.

[8] **Brown, G. D., Herre, J., Williams, D. L., Willment, J. A., Marshall, A. S. and Gordon, S.,** Dectin-1 mediates the biological effects of beta-glucans. *J Exp Med* 2003. **197**: 1119-1124.

[9] **Shah, V. B., Huang, Y., Keshwara, R., Ozment-Skelton, T., Williams, D. L. and Keshvara, L.,** Beta-glucan activates microglia without inducing cytokine production in Dectin-1-dependent manner. *J Immunol* 2008. **180**: 2777-2785.

[10] **Dennehy, K. M., Ferwerda, G., Faro-Trindade, I., Pyz, E., Willment, J. A., Taylor, P. R., Kerrigan, A.et al.,** Syk kinase is required for collaborative cytokine production induced through Dectin-1 and Toll-like receptors. *Eur J Immunol* 2008. **38**: 500-506.

[11] **Walachowski, S., Tabouret, G. and Foucras, G.,** Triggering Dectin-1-Pathway Alone Is Not Sufficient to Induce Cytokine Production by Murine Macrophages. *PloS one* 2016. **11**: e0148464.

[12] **Goodridge, H. S., Shimada, T., Wolf, A. J., Hsu, Y. M., Becker, C. A., Lin, X. and Underhill, D. M.,** Differential use of CARD9 by dectin-1 in macrophages and dendritic cells. *J Immunol* 2009. **182**: 1146-1154.

[13] **Hernanz-Falcon, P., Joffre, O., Williams, D. L. and Reis e Sousa, C.,** Internalization of Dectin-1 terminates induction of inflammatory responses. *Eur J Immunol* 2009. **39**: 507-513.

[14] **Rosas, M., Liddiard, K., Kimberg, M., Faro-Trindade, I., McDonald, J. U., Williams, D. L., Brown, G. D.et al.,** The induction of inflammation by dectin-1 in vivo is dependent on myeloid cell programming and the progression of phagocytosis. *J Immunol* 2008. **181**: 3549-3557.

[15] **LeibundGut-Landmann, S., Gross, O., Robinson, M. J., Osorio, F., Slack, E. C., Tsoni, S. V., Schweighoffer, E.et al.,** Syk- and CARD9-dependent coupling of innate immunity to the induction of T helper cells that produce interleukin 17. *Nat Immunol* 2007. **8**: 630-638.

[16] **Yoshitomi, H., Sakaguchi, N., Kobayashi, K., Brown, G. D., Tagami, T., Sakihama, T., Hirota, K.et al.,** A role for fungal {beta}-glucans and their receptor Dectin-1 in the induction of autoimmune arthritis in genetically susceptible mice. *J Exp Med* 2005. **201**: 949-960.

[17] **Auffray, C., Sieweke, M. H. and Geissmann, F.,** Blood monocytes: development, heterogeneity, and relationship with dendritic cells. *Annu Rev Immunol* 2009. **27**: 669-692.

[18] **Ginhoux, F. and Jung, S.,** Monocytes and macrophages: developmental pathways and tissue homeostasis. *Nat Rev Immunol* 2014. **14**: 392-404.

[19] **Shi, C. and Pamer, E. G.,** Monocyte recruitment during infection and inflammation. *Nat Rev Immunol* 2011. **11**: 762-774.

[20] **Saeed, S., Quintin, J., Kerstens, H. H., Rao, N. A., Aghajanirefah, A., Matarese, F., Cheng, S. C.et al.,** Epigenetic programming of monocyte-to-macrophage differentiation and trained innate immunity. *Science* 2014. **345**: 1251086.

[21] **van der Meer, J. W., Joosten, L. A., Riksen, N. and Netea, M. G.,** Trained immunity: A smart way to enhance innate immune defence. *Mol Immunol* 2015. **68**: 40-44.

[22] **Bain, J. M., Louw, J., Lewis, L. E., Okai, B., Walls, C. A., Ballou, E. R., Walker, L. A.et al.,** Candida albicans hypha formation and mannan masking of beta-glucan inhibit macrophage phagosome maturation. *MBio* 2014. **5**: e01874.

[23] **Gow, N. A., van de Veerdonk, F. L., Brown, A. and Netea, M. G.,** Candida albicans morphogenesis and the host defence: discriminating invasion from colonization. *Nat Rev Microbiol* 2012. **10**: 112-122.

[24] **Broz, P. and Dixit, V. M.,** Inflammasomes: mechanism of assembly, regulation and signalling. *Nat Rev Immunol* 2016. **16**: 407-420.

[25] **Gaidt, M. M., Ebert, T. S., Chauhan, D., Schmidt, T., Schmid-Burgk, J. L., Rapino, F., Robertson, A. A.et al.,** Human Monocytes Engage an Alternative Inflammasome Pathway. *Immunity* 2016. **44**: 833-846.

[26] **Hogquist, K. A., Nett, M. A., Unanue, E. R. and Chaplin, D. D.,** Interleukin 1 is processed and released during apoptosis. *Proc Natl Acad Sci U S A* 1991. **88**: 8485-8489.

[27] **Kayagaki, N., Warming, S., Lamkanfi, M., Vande Walle, L., Louie, S., Dong, J., Newton, K.et al.,** Non-canonical inflammasome activation targets caspase-11. *Nature* 2011. **479**: 117-121.

[28] **Shi, J., Zhao, Y., Wang, Y., Gao, W., Ding, J., Li, P., Hu, L.et al.,** Inflammatory caspases are innate immune receptors for intracellular LPS. *Nature* 2014. **514**: 187-192.

[29] **Vigano, E., Diamond, C. E., Spreafico, R., Balachander, A., Sobota, R. M. and Mortellaro, A.,** Human caspase-4 and caspase-5 regulate the one-step non-canonical inflammasome activation in monocytes. *Nat Commun* 2015. **6**: 8761.

[30] **Gringhuis, S. I., Kaptein, T. M., Wevers, B. A., Theelen, B., van der Vlist, M., Boekhout, T. and Geijtenbeek, T. B.,** Dectin-1 is an extracellular pathogen sensor for the induction and processing of IL-1beta via a noncanonical caspase-8 inflammasome. *Nat Immunol* 2012. **13**: 246-254.

[31] **Ganesan, S., Rathinam, V. A., Bossaller, L., Army, K., Kaiser, W. J., Mocarski, E. S., Dillon, C. P.et al.,** Caspase-8 modulates dectin-1 and complement receptor 3-driven IL-1beta production in response to beta-glucans and the fungal pathogen, Candida albicans. *J Immunol* 2014. **193**: 2519-2530.

[32] **Tzeng, T. C., Schattgen, S., Monks, B., Wang, D., Cerny, A., Latz, E., Fitzgerald, K.et al.,** A Fluorescent Reporter Mouse for Inflammasome Assembly Demonstrates an Important Role for Cell-Bound and Free ASC Specks during In Vivo Infection. *Cell Rep* 2016. **16**: 571-582.

[33] **Gurung, P., Burton, A. and Kanneganti, T. D.,** NLRP3 inflammasome plays a redundant role with caspase 8 to promote IL-1beta-mediated osteomyelitis. *Proc Natl Acad Sci U S A* 2016. **113**: 4452-4457.

[34] **Schmitt, A., Grondona, P., Maier, T., Brandle, M., Schonfeld, C., Jager, G., Kosnopfel, C.et al.,** MALT1 Protease Activity Controls the Expression of Inflammatory Genes in Keratinocytes upon Zymosan Stimulation. *The Journal of investigative dermatology* 2016. **136**: 788-797.

[35] **Netea, M. G., Brown, G. D., Kullberg, B. J. and Gow, N. A.,** An integrated model of the recognition of Candida albicans by the innate immune system. *Nat Rev Microbiol* 2008. **6**: 67-78.

[36] **Bose, N., Wurst, L. R., Chan, A. S., Dudney, C. M., LeRoux, M. L., Danielson, M. E., Will, P. M.et al.,** Differential regulation of oxidative burst by distinct beta-glucan-binding receptors and signaling pathways in human peripheral blood mononuclear cells. *Glycobiology* 2014. **24**: 379-391.

[37] **Drummond, R. A., Saijo, S., Iwakura, Y. and Brown, G. D.,** The role of Syk/CARD9 coupled C-type lectins in antifungal immunity. *Eur J Immunol* 2011. **41**: 276-281.

[38] **Shah, V. B., Ozment-Skelton, T. R., Williams, D. L. and Keshvara, L.,** Vav1 and PI3K are required for phagocytosis of beta-glucan and subsequent superoxide generation by microglia. *Mol Immunol* 2009. **46**: 1845-1853.

[39] **Kawai, T. and Akira, S.,** The roles of TLRs, RLRs and NLRs in pathogen recognition. *Int Immunol* 2009. **21**: 317-337.

[40] **Blanco-Menendez, N., del Fresno, C., Fernandes, S., Calvo, E., Conde-Garrosa, R., Kerr, W. G. and Sancho, D.,** SHIP-1 Couples to the Dectin-1 hemITAM and Selectively Modulates Reactive Oxygen Species Production in Dendritic Cells in Response to Candida albicans. *J Immunol* 2015. **195**: 4466-4478.

[41] **Filler, S. G., Pfunder, A. S., Spellberg, B. J., Spellberg, J. P. and Edwards, J. E., Jr.,** Candida albicans stimulates cytokine production and leukocyte adhesion molecule expression by endothelial cells. *Infect Immun* 1996. **64**: 2609-2617.

[42] **Boxx, G. M., Kozel, T. R., Nishiya, C. T. and Zhang, M. X.,** Influence of mannan and glucan on complement activation and C3 binding by Candida albicans. *Infect Immun* 2010. **78**: 1250-1259.

[43] **Elder, M. J., Webster, S. J., Chee, R., Williams, D. L., Hill Gaston, J. S. and Goodall, J. C.,** β-Glucan Size Controls Dectin-1-Mediated Immune Responses in

Human Dendritic Cells by Regulating IL-1 β Production. *Frontiers in immunology* 2017. **8**.

[44] **Warnatsch, A., Tsourouktsoglou, T. D., Branzk, N., Wang, Q., Reincke, S., Herbst, S., Gutierrez, M.et al.,** Reactive Oxygen Species Localization Programs Inflammation to Clear Microbes of Different Size. *Immunity* 2017. **46**: 421-432.

[45] **Said-Sadier, N., Padilla, E., Langsley, G. and Ojcius, D. M.,** Aspergillus fumigatus stimulates the NLRP3 inflammasome through a pathway requiring ROS production and the Syk tyrosine kinase. *PloS one* 2010. **5**: e10008.

[46] **Lowman, D. W., Greene, R. R., Bearden, D. W., Kruppa, M. D., Pottier, M., Monteiro, M. A., Soldatov, D. V.et al.,** Novel structural features in Candida albicans hyphal glucan provide a basis for differential innate immune recognition of hyphae versus yeast. *J Biol Chem* 2014. **289**: 3432-3443.

[47] **Joly, S., Ma, N., Sadler, J. J., Soll, D. R., Cassel, S. L. and Sutterwala, F. S.,** Cutting edge: Candida albicans hyphae formation triggers activation of the Nlrp3 inflammasome. *J Immunol* 2009. **183**: 3578-3581.

[48] **Mukaremera, L., Lee, K. K., Mora-Montes, H. M. and Gow, N. A. R.,** Candida albicans Yeast, Pseudohyphal, and Hyphal Morphogenesis Differentially Affects Immune Recognition. *Frontiers in immunology* 2017. **8**: 629.

[49] **Bonhomme, J. and d'Enfert, C.,** Candida albicans biofilms: building a heterogeneous, drug-tolerant environment. *Curr Opin Microbiol* 2013. **16**: 398-403.

[50] **Alonso, M. F., Gow, N. A., Erwig, L. P. and Bain, J. M.,** Macrophage Migration Is Impaired within Candida albicans Biofilms. *J. Fungi* 2017. **3**: 31.

[51] **Aimanianda, V., Clavaud, C., Simenel, C., Fontaine, T., Delepierre, M. and Latge, J. P.,** Cell wall beta-(1,6)-glucan of Saccharomyces cerevisiae: structural characterization and in situ synthesis. *J Biol Chem* 2009. **284**: 13401-13412.

[52] **Aimanianda, V., Simenel, C., Garnaud, C., Clavaud, C., Tada, R., Barbin, L., Mouyna, I.et al.,** The Dual Activity Responsible for the Elongation and Branching of beta-(1,3)-Glucan in the Fungal Cell Wall. *MBio* 2017. **8**.

[53] **Stephen-Victor, E., Karnam, A., Fontaine, T., Beauvais, A., Das, M., Hegde, P., Prakhar, P.et al.,** Aspergillus fumigatus cell wall alpha-(1,3)-glucan stimulates regulatory T cell polarization by inducing PD-L1 expression on human dendritic cells. *J Infect Dis* 2017.

Figure legends

Figure 1. Effects of phagocytosis impairment on the response of human monocytes towards whole *Candida albicans* and the cell wall fraction composed of branched β-glucan. (A-B) Human monocytes were left untreated (ctrl) or stimulated with either heat-killed *Candida albicans* (HK-C.a., A) or heat-killed *Saccharomyces cerevisiae* (HK-S.c., B) in the presence (Cyt D) or in the absence (DMSO) of cytochalasin D. (C) Cells were stimulated with the Alkali-Soluble (AS) and Insoluble (AI) fractions, β-(1-6)-glucan and β-(1-3)/(1-6) glucan fractions from the cell wall of *Saccharomyces cerevisiae* after being treated with DMSO or Cyt D. (D) Data show the stimulation experiments of monocytes with two doses (1 or 10 μg/ml) of branched β-(1-3)-glucan isolated from *C. albicans* (β-glucan C.a.) or from *S. cerevisiae* (β-glucan S.c.) in the presence or in the absence of Cyt D. (E) Data show the stimulation experiments of monocytes with two doses (1 or 10 μg/ml) of insoluble linear β-(1-3)-glucan (curdlan) or of soluble branched β-(1-3)-glucan (laminarin) in the presence or in the absence of Cyt D. (F) The particulate branched β-(1-3)-glucan isolated from the cell wall of *C. albicans* was sonicated (Sonifier cell Disruptor B-30. Outputcontrol 4, Duty cycle 40%; 2 times 10 cycle with 5min on ice in between the two sets). Monocytes were then exposed to either sonicated or not-sonicated β–glucan in the presence or in the absence of Cyt D. (G) Cells pre-treated with DMSO or Cyt D were stimulated for 24h with the indicated concentrations of β-glucan from *C. albicans* (β-glucan C.a.), HK-C.a., AS and AI fractions from S.c., or the combination of AS+AI (10+10 μg/ml). (H) Monocytes were pre-treated with either DMSO (control), or with cytochalasin D (Cyt D) or latrunculin B (Lat B) (actin polymerization inhibitors), or with jasplakinolide (Jsp, actin polymerization inducer), or with chlorpromazine (CLP, clathrin-mediated endocytic inhibitor) or the lysosomal inhibitor cloroquine (CLQ). Cells were then stimulated with either branched β-(1-3)-glucan isolated

from *C. albicans* (β -glucan C.a.) or with heat-killed *Candida albicans* (HK-C.a.). For all the experiments, culture supernatants were collected after 24h and concentration of secreted TNFα, IL6, IL1β and IL10 was determined by ELISA. Data were reproducible for all the four cytokines tested even if histograms are not shown. Graphs show the mean ± SEM of at least three independent experiments. For (A, H), n = 8; for (B-G), n = 6; *p < 0.05, **p < 0.01. Wilcoxon matched-pairs signed-rank test.

Figure 2. The role of the NLRP3-ASC-caspase-1 inflammasome in β-glucan induced IL1β. (A and E) Monocytes were pre-treated with either z-VAD-fmk (pan-caspase inhibitor), z-YVAD-fmk (caspase-1 inhibitor), z-IETD-fmk (caspase-8 inhibitor), z-LEVD-fmk (caspase-4/5 inhibitor), MCC950 (NLRP3 inhibitor), glibenclamide (inhibitor of potassium (K+) efflux) or z-VRPR-fmk (MALT1 inhibitor) before treatment with either DMSO or Cyt D for 1h. Cells were then stimulated with branched β-(1-3)-glucan isolated from *C. albicans* (β-glucan C.a.), culture supernatants were collected after 24h and secretion of IL1β was determined by ELISA. Graphs show the mean ± SEM of four independent experiments (n=8). **P < 0.001 (B) Monocytes were stimulated for 6h with or without β–glucan C.a. in the presence or absence of Cyt D, as indicated. Caspase-1 (pro-form and cleaved p20), NLRP3 and IL1β (pro- and mature IL1β) expression was assessed by western blot. Arrows indicate the specific band for NLRP3 and the mature and active form of IL1β and caspase-1, respectively. GAPDH was used as the loading control. Blots are representative of three independent experiments. (C) Immunofluorescence microscopy of ASC inflammasomes. Representative images of monocytes stimulated for 6h with or without β-glucan C.a. in the presence or absence of Cyt D and stained with Hoechst in blue (DNA) and ASC in red. Original magnification. 60x, Scale Bar: 50μm. (D) Quantification of the percentage ASC

specks from (C) (3x200 cells analysed with Image J). *P < 0.05 and **P < 0.01; 2-tailed Student's t test.

Figure 3. The role of the Dectin-1/Syk/PI3K pathway in the overproduction of cytokines by monocytes impaired for phagocytosis and stimulated with β-glucan. Monocytes were pre-treated with anti-Dectin-1 Ab, anti-TLR2 Ab, anti-CR3 Ab or isotype control Abs in (A). Syk inhibitor in (B), or PI3K inhibitor (WRT; wortmannin) in (C), were used on monocytes as indicated. After the first incubation with inhibitors, cells were treated either with DMSO or Cyt D and finally stimulated with branched β-(1-3)-glucan isolated from *C. albicans* (β-glucan C.a.). Culture supernatants were collected after 24h and secretion of TNFα, IL6 and IL1β was determined by ELISA. Graphs show the mean ± SEM of at least three independent experiments. For (A), n = 6; for (B) and (C), n = 9; *p < 0.05, **p < 0.01. Wilcoxon matched-pairs signed-rank test.

Figure 4. IκBα phosphorylation, IκBα degradation and p65 nuclear translocation in cytochalasin D/β-glucan stimulated monocytes. (A) Western blot analysis of phospho-IκBα and IκBα in cell lysates from monocytes treated for 6h with or without β–glucan C.a. in the presence or absence of Cyt D. GAPDH was used as a loading control. (B) Graphs represent the densitometric analysis of the blots. Immunoreactive bands were normalized to GAPDH. The bars represent mean values ± SEM of the analysis of 4 independent experiments. (C) Cells were treated as in (A) and nuclear translocation of p65 NF-κB was visualized by immunostaining with a specific antibody recognizing p65 and an alexa-fluor 488-conjugated secondary antibody (green). For reference the nuclei are stained Hoescht (blue). One representative image of three independent experiments is shown. (D) Quantification of nuclei

with p65 translocation (3x200 nuclei analysed with Image J). Original magnification. 60x, scale bar: 50μM. *P < 0.05 and **P < 0.01; 2-tailed Student's t test.

Figure 5. Analysis of ROS production in human monocytes with impaired phagocytosis mechanism upon β-glucan stimulation. Monocytes were pre-treated for 30 min with (A) the indicated concentrations of DPI (NADPH oxidase inhibitor) before being treated with either DMSO or Cyt D for 1h. Cells were then left untreated or stimulated with particulate β–glucan C.a.. Luminol was added, and Reactive oxygen species (ROS) production was monitored by chemiluminescence during time (2h) and expressed as relative light units (RLU). Graphs show mean ± SEM corresponding to up to three independent experiments (n=3); each experimental condition was assessed in triplicate. (B) Monocytes were pre-treated with DPI, as indicated. After 30 min of incubation, cells were treated either with DMSO or Cyt D and, after an additional 1h, stimulated with β-glucan C.a.. Culture supernatants were collected after 24h and secretion of TNFα, IL6 and IL1β was determined by ELISA. Graphs show the mean + SEM of at least three independent experiments (n = 8); **p < 0.01. Wilcoxon matched-pairs signed-rank test. (C-D) For inhibition, monocytes were pre-incubated for 30 min with the vehicle (control), Syk inhibitor (2 μM), anti-Dectin-1 Ab, or PI3K inhibitor (wortmannin) and then treated as in (A). ROS production was monitored by chemiluminescence. Graphs show mean + SEM corresponding to three independent experiments (n=5); each experimental condition was assessed in duplicate or triplicate depending on the number of cells available. (D) RLU data are plotted as histograms of mean + SEM of the maximal ROS production corresponding to three independent experiments (n = 5). Significant synergy is represented as # p<0,05, ## p<0,01. *P < 0.05, **P < 0.01and ***P < 0.001; one-way ANOVA.

Figure 6. Syk activity assessement for inflammasome, and NF-κB activation in phagocytosis-impaired-monocyte stimulated with *C. albicans*-branched β-(1-3)-glucan. (A) Monocytes treated for 6h with β–glucan C.a. in the presence or absence of Cyt D and of the Syk inhibitor (2 μM). Nuclear translocation of p65 NF-κB was visualized by immunostaining with a specific antibody recognizing p65 and a alexa-fluor 488-conjugated secondary antibody (green). For reference the nuclei are stained Hoescht (blue). Original magnification. 60x, scale bar: 50μM Image is representative of three independent experiments. (B) Quantification of nuclei with p65 translocation (4x50 nuclei analysed with Image J). (C) Cells were treated as in (A). Caspase-1 (pro-form and cleaved p20), and IL1β (pro- and mature IL1β) expressions were assessed by western blot. Mature IL1β and caspase-1 were also detected in cell culture supernatants. GAPDH was used as the loading control. Blots are representative of three independent experiments.

Figure 7. Schematic model illustrating potential signaling pathways triggered by the binding of β–glucan to dectin-1 in human monocytes with normal (left) or impaired phagocytic (right) function. Attenuation of dectin-1 signaling is associated with the engulfment of the receptor/ligand complex. By contrast, blocking of actin-dependent phagocytosis led to increased cell activation. Black lines depict the interactions that normally occur upon phagocytosis and β–glucan/dectin-1 interaction, whereas red lines indicate the proposed signaling events that enhance the strength and efficacy of signal propagation.

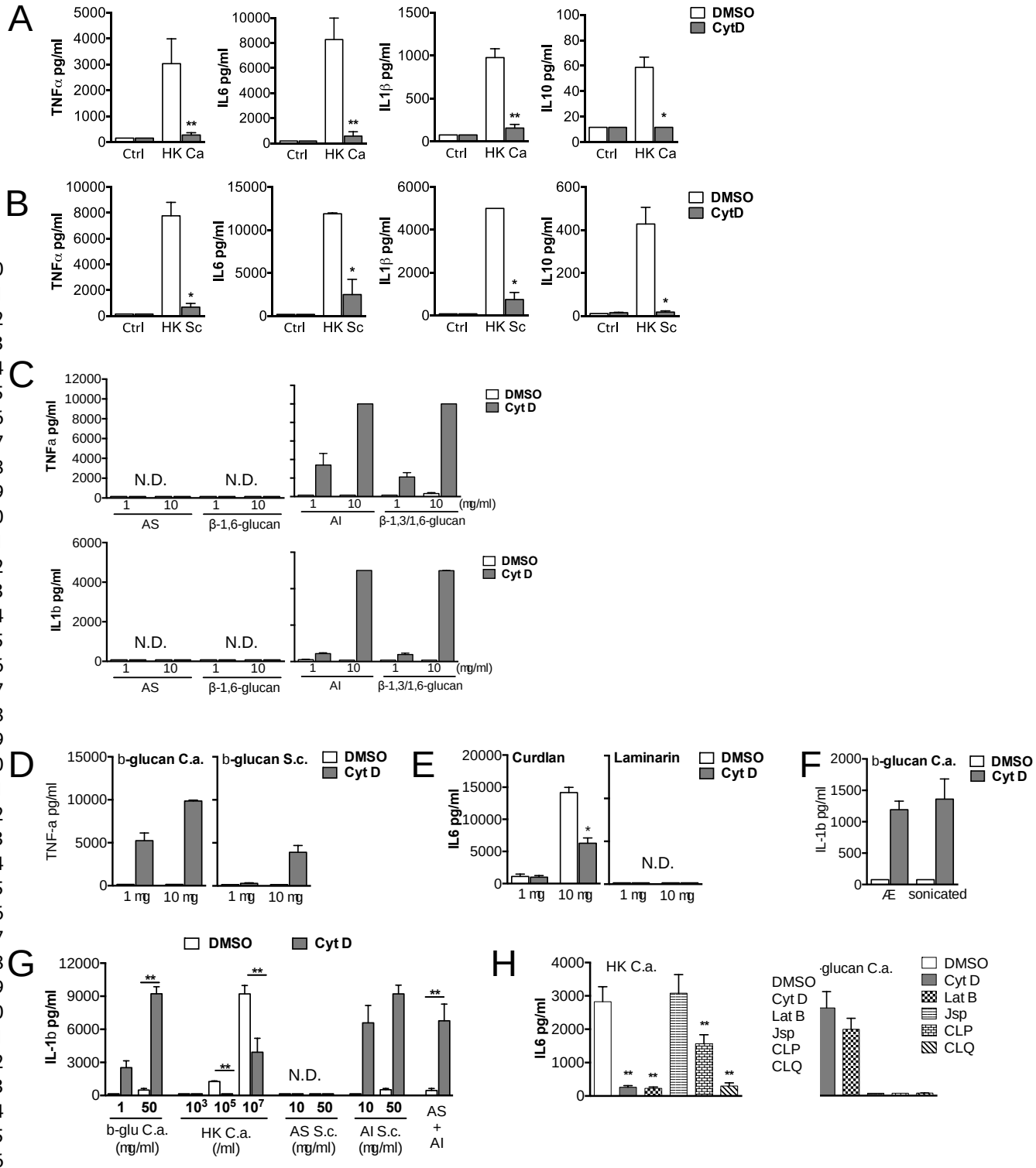
A
TNFα pg/ml
IL6 pg/ml
IL1β pg/ml
IL10 pg/ml
Ctrl
HK Ca
DMSO
CytD
B
HK Sc
C
TNFa pg/ml
IL1b pg/ml
N.D.
AS
β-1,6-glucan
AI
β-1,3/1,6-glucan
(mg/ml)
Cyt D
D
b-glucan C.a.
b-glucan S.c.
TNF-a pg/ml
1 mg
10 mg
E
Curdlan
Laminarin
IL6 pg/ml
F
IL-1b pg/ml
Æ
sonicated
G
IL-1b pg/ml
b-glu C.a. (mg/ml)
HK C.a. (/ml)
AS S.c. (mg/ml)
AI S.c. (mg/ml)
AS + AI
H
HK C.a.
glucan C.a.
Lat B
Jsp
CLP
CLQ

Figure 1

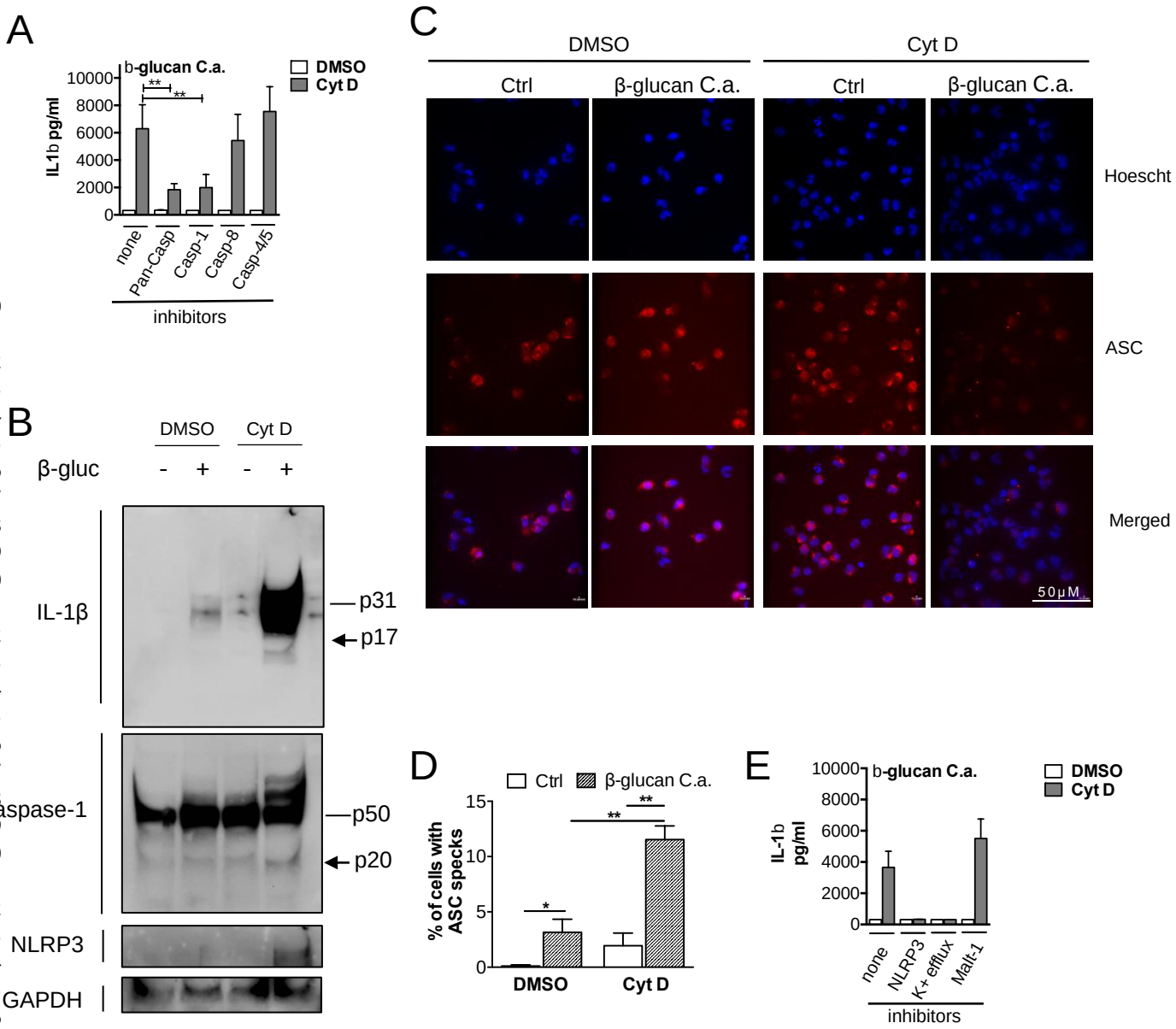
A
b-glucan C.a.
DMSO
Cyt D
IL1b pg/ml
10000
8000
6000
4000
2000
0
**
**
none
Pan-Casp
Casp-1
Casp-8
Casp-4/5
inhibitors
B
DMSO
Cyt D
β-gluc
- + - +
IL-1β
p31
p17
Caspase-1
p50
p20
NLRP3
GAPDH
C
DMSO
Cyt D
Ctrl
β-glucan C.a.
Ctrl
β-glucan C.a.
Hoescht
ASC
Merged
50µM
D
Ctrl
β-glucan C.a.
% of cells with ASC specks
15
10
5
0
*
**
**
DMSO
Cyt D
E
b-glucan C.a.
DMSO
Cyt D
IL-1b pg/ml
10000
8000
6000
4000
2000
0
none
NLRP3
K+ efflux
Malt-1
inhibitors

Figure 2

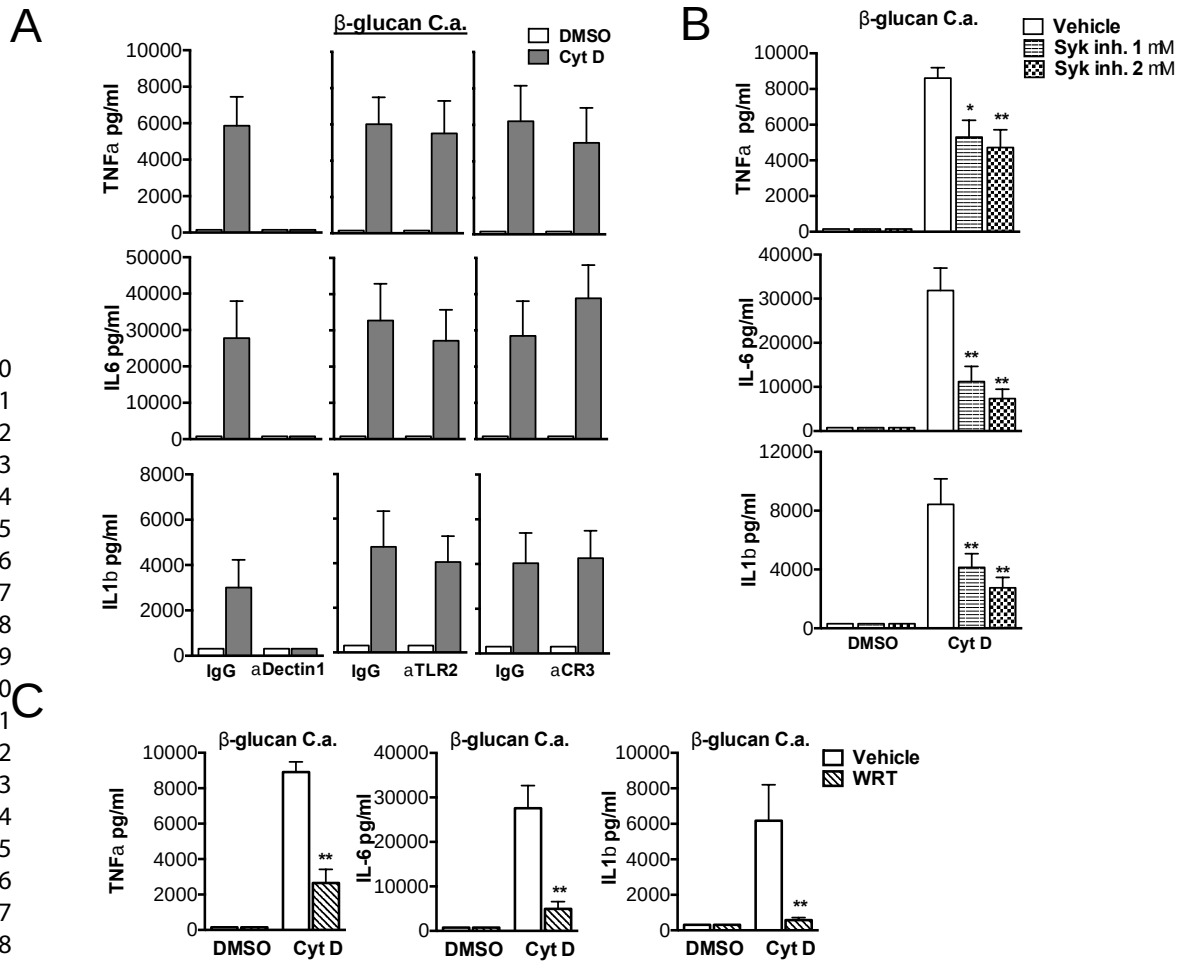
A
β-glucan C.a.
DMSO
Cyt D
TNFa pg/ml
IL6 pg/ml
IL1b pg/ml
IgG
aDectin1
IgG
aTLR2
IgG
aCR3
B
β-glucan C.a.
Vehicle
Syk inh. 1 mM
Syk inh. 2 mM
TNFa pg/ml
IL-6 pg/ml
IL1b pg/ml
DMSO
Cyt D
C
β-glucan C.a.
TNFa pg/ml
β-glucan C.a.
IL-6 pg/ml
β-glucan C.a.
IL1b pg/ml
Vehicle
WRT
DMSO
Cyt D

Figure 3

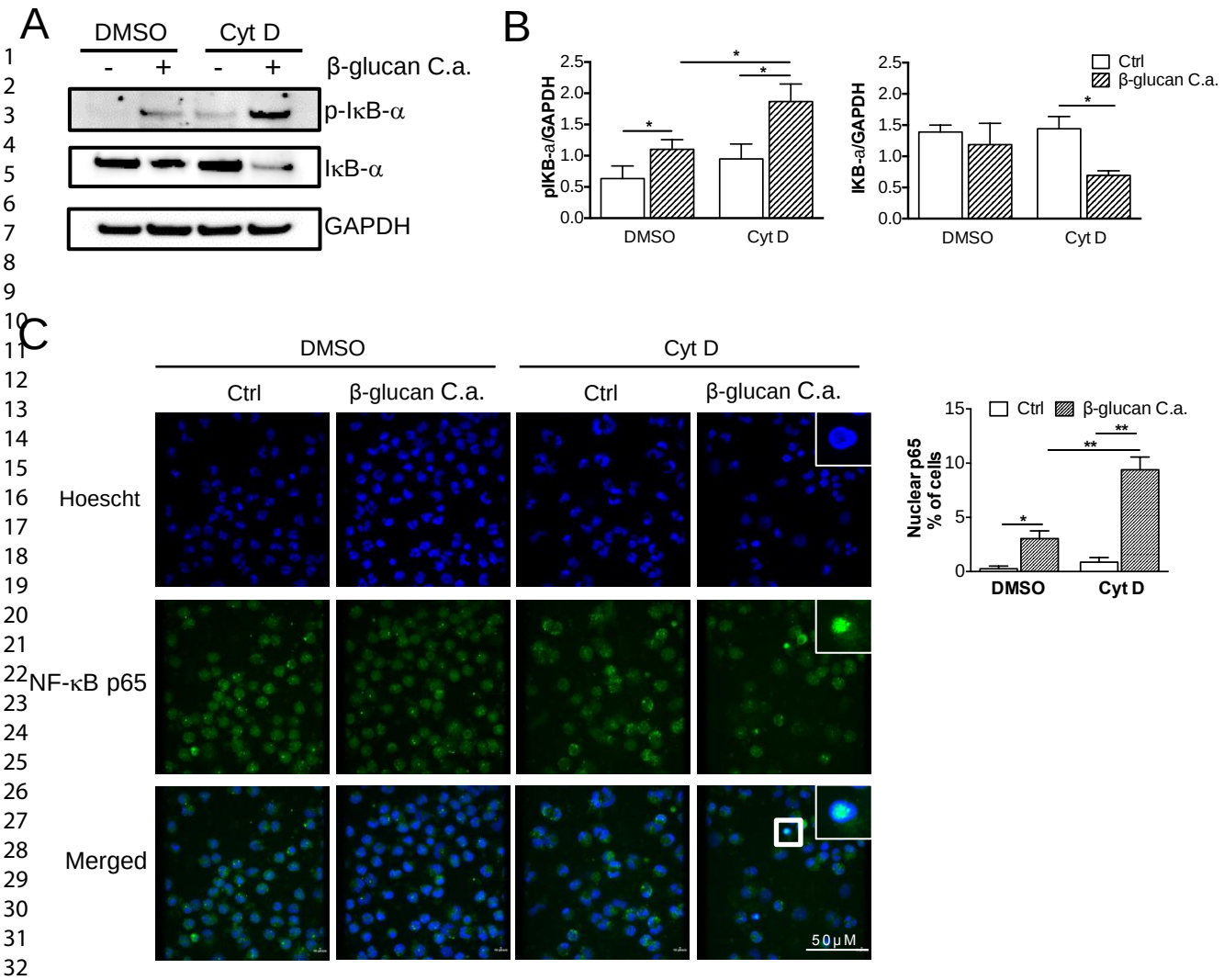
A
DMSO
Cyt D
- + - +
β-glucan C.a.
p-IκB-α
IκB-α
GAPDH
B
pIKB-a/GAPDH
2.5
2.0
1.5
1.0
0.5
0.0
DMSO
Cyt D
IKB-a/GAPDH
Ctrl
β-glucan C.a.
C
DMSO
Cyt D
Ctrl
β-glucan C.a.
Hoescht
NF-κB p65
Merged
50µM
Nuclear p65
% of cells
15
10
5
0

Figure 4

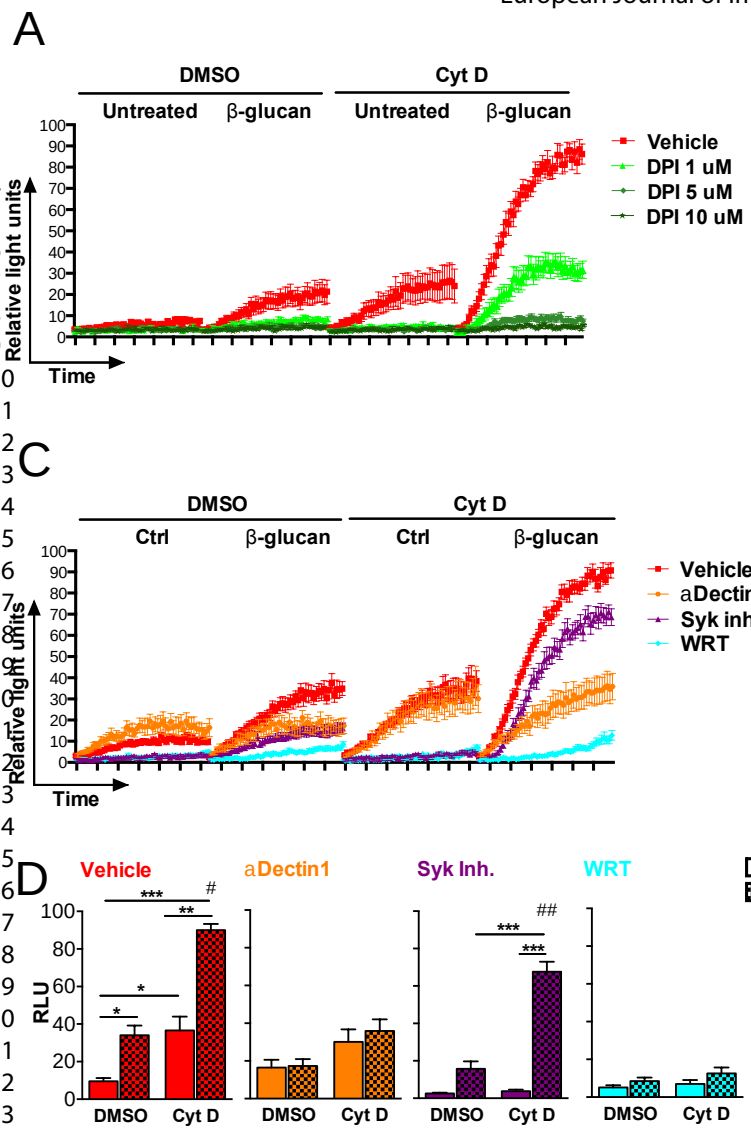
A
DMSO
Cyt D
Untreated
β-glucan
Untreated
β-glucan
Relative light units
Time
Vehicle
DPI 1 uM
DPI 5 uM
DPI 10 uM
C
DMSO
Cyt D
Ctrl
β-glucan
Ctrl
β-glucan
Relative light units
Time
Vehicle
aDectin1
Syk inh.
WRT
D
Vehicle
aDectin1
Syk Inh.
WRT
RLU
DMSO
Cyt D
Ctrl
β-glucan C.a.

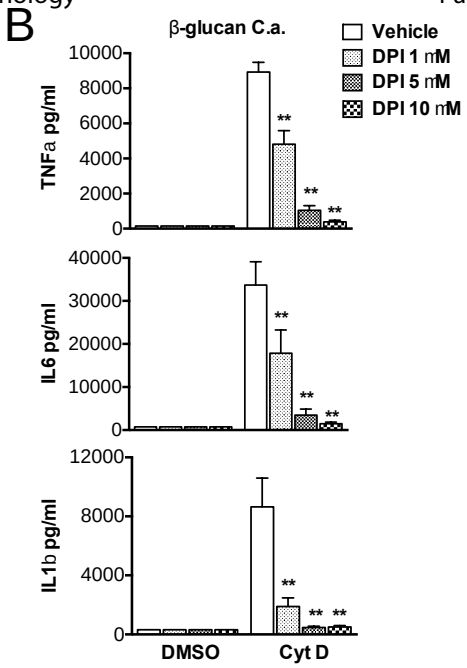
B
β-glucan C.a.
Vehicle
DPI 1 mM
DPI 5 mM
DPI 10 mM
TNFa pg/ml
IL6 pg/ml
IL1b pg/ml
DMSO
Cyt D

Figure 5

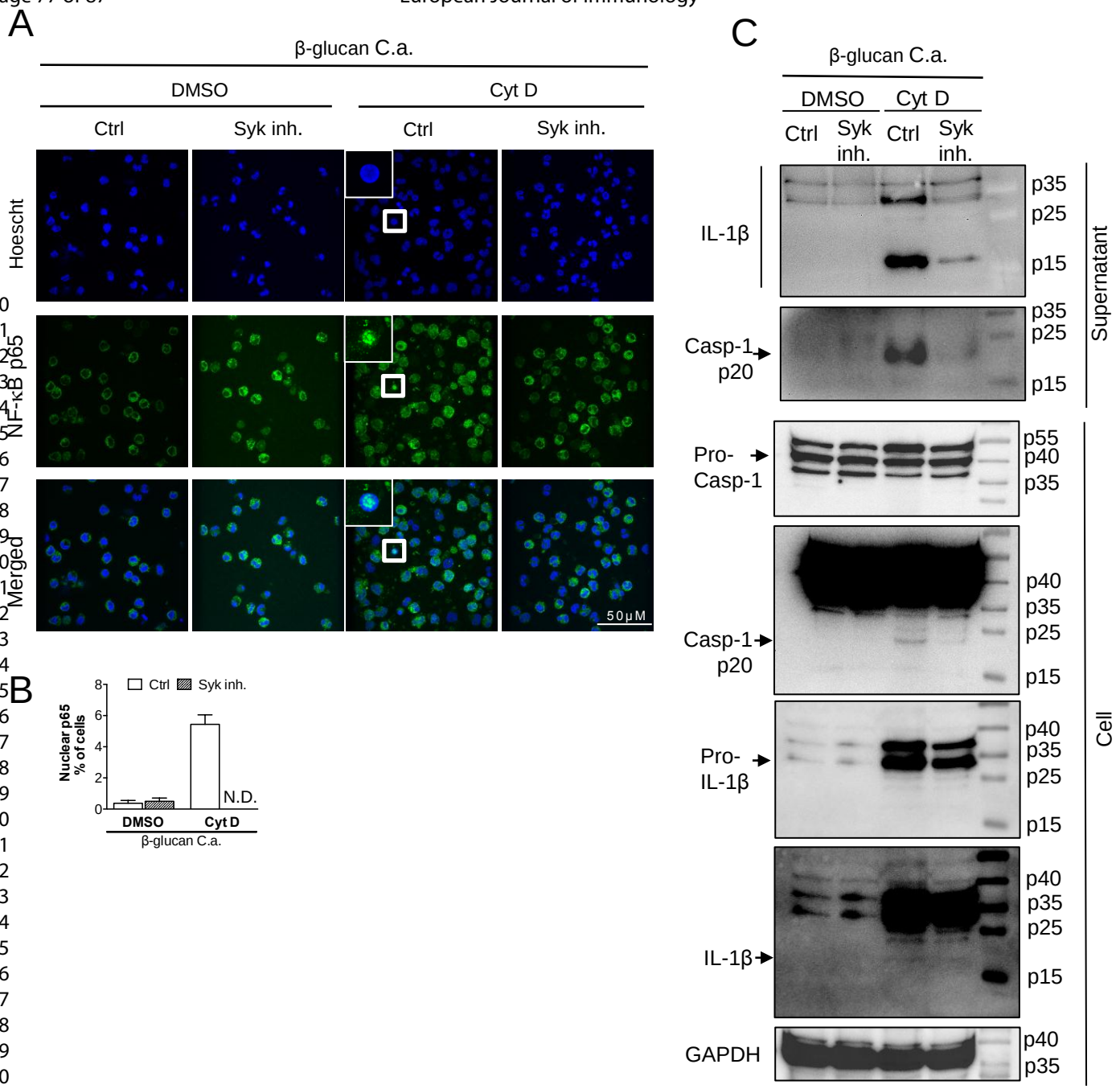
A
β-glucan C.a.
DMSO
Cyt D
Ctrl
Syk inh.
Ctrl
Syk inh.
Hoescht
NF-κB p65
Merged
50μM
B
Ctrl
Syk inh.
Nuclear p65
% of cells
8
6
4
2
0
N.D.
DMSO
Cyt D
β-glucan C.a.
C
β-glucan C.a.
DMSO
Cyt D
Ctrl
Syk inh.
Ctrl
Syk inh.
IL-1β
p35
p25
p15
Supernatant
Casp-1
p20
p35
p25
p15
Pro-
Casp-1
p55
p40
p35
Casp-1
p20
p40
p35
p25
p15
Cell
Pro-
IL-1β
p40
p35
p25
p15
IL-1β
p40
p35
p25
p15
GAPDH
p40
p35

Figure 6

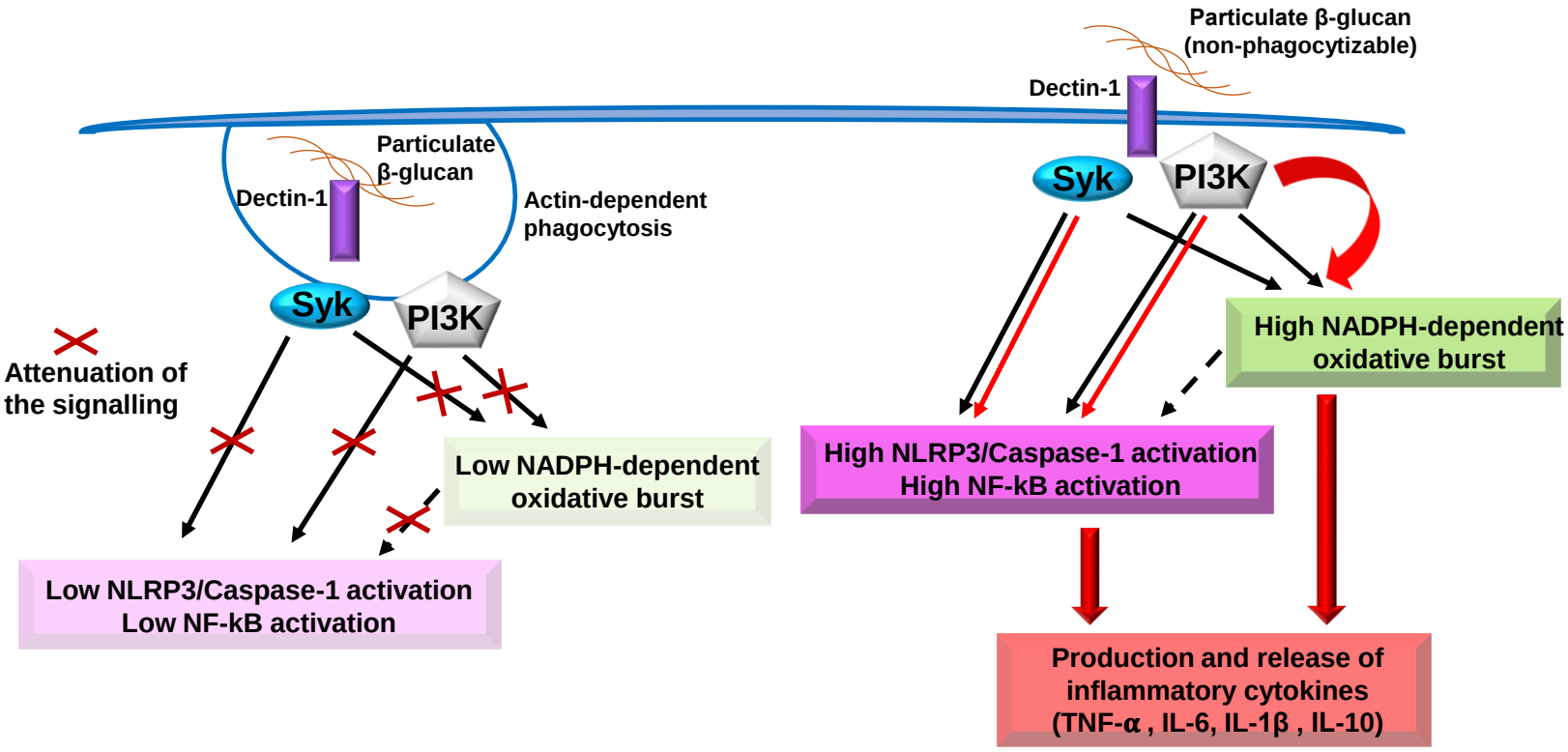
Particulate β-glucan
(non-phagocytizable)
Dectin-1
Syk
PI3K
High NADPH-dependent
oxidative burst
High NLRP3/Caspase-1 activation
High NF-kB activation
Production and release of
inflammatory cytokines
(TNF-α , IL-6, IL-1β , IL-10)
Particulate
β-glucan
Dectin-1
Actin-dependent
phagocytosis
Syk
PI3K
Attenuation of
the signalling
Low NADPH-dependent
oxidative burst
Low NLRP3/Caspase-1 activation
Low NF-kB activation

Figure 7

Supporting Information

Supporting Information Figure 1. Internalization of FITC–labelled heat-killed *C. albicans* or β-glucans from *C. albicans* or from *S. cerevisiae* or curdlan, by monocytes in the presence or in the absence of cytochalasin D. Extracellular fluorescence is left unquenched or quenched by trypan blue. Original magnification, x20.

Supporting Information Figure 2. Differential Interference Contrast (DIC) of pure monocytes incubated with or without *C. albicans*-branched β-(1,3)-glucan in the presence or absence of Cytochalasin D (CytD). No aggregates of β-glucan can be observed with or without CytD. It is rather a network of external filaments of β-(1,3)-glucan that can be observed in the right bottom left, when phagocytosis is impaired. Original magnification, x20.

Supporting Information Figure 3. Monocytes were pre-treated with a cocktail of 3 anti-CR3 antibodies (3x αCR3) or isotype controls as described in Materials and Methods. After the first 30 min incubation with the anti-CR3 antibodies cocktail, cells were treated for 1h either with DMSO or Cyt D and finally stimulated with branched β-(1,3)-glucan isolated from *C. albicans* (β-glucan C.a.). Culture supernatants were collected after 24h and secretion of TNF-α, IL-6 and IL-1β was determined by ELISA. Graphs show the mean ± SEM of at least three independent experiments, n = 10; *$p < 0.05$.

Supporting Information Figure 4. Analysis of Cyt D plus β–glucan C.a.-induced oxidative burst and cytokine production in the presence of NADPH oxidases inhibitor apocynin. (A) Monocytes were pre-treated for 30 min with the vehicle (control) or apocynin (Apo; NADPH oxidase inhibitor) before being treated with either DMSO or Cyt D for 1h. Cells were then left

untreated or stimulated with particulate β–glucan C.a.. Luminol was added, ROS production was monitored by chemiluminescence during time (2h) and expressed as relative light units. Graphs show mean ± SEM corresponding to up to three independent experiments. For each condition, values were normalized to the average reading of the untreated control (DMSO/Untreated/Vehicle). (B) Cells were treated as in (A), culture supernatants were collected after 24h and secretion of TNF-α, IL-6 and IL-1β was determined by ELISA. Graphs show the mean ± SEM of three independent experiments (n = 6). *$p < 0.05$; **$p < 0.01$.

Supporting Information Figure 5. Lactate dehydrogenase cytotoxicity assay for monocytes after exposure to several inhibitors. Cells were pre-incubated for 30 min with the indicated inhibitors before stimulation for 24h with Cyt D (1 μg/ml) + β-glucan C.a. (1 μg/ml). The results were normalized to the maximum LDH release and expressed as fold change compared to control cells. Graphs show the mean +/- SEM of at least three independent experiments. **$p < 0.01$ and ***$p < 0.001$ versus control (none); one-way ANOVA.

Supporting Information Figure 6. (A) Monocytes were pre-treated for 30 min with either z-LEVD-fmk (caspase-4/5 inhibitor) or z-YVAD-fmk (caspase-1 inhibitor) before treatment with LPS (10 ng/ml) (LPS-EB Ultrapure, InvivoGen) for 24h. In (B), cells were pre-treated with z-VRPR-fmk (MALT1 inhibitor) before stimulation with HK-C.a. (10^5/ml) for 24h. Culture supernatants were collected and secretion of IL-1β was determined by ELISA. Graphs show the mean ± SEM of four independent experiments (n=7). *$P < 0.05$ and **$P < 0.01$. (C) macrophages were stimulated with z-IETD-fmk (caspase-8 inhibitor) or LPS (200ng/mL) alone or in combination. IL-1β release and cell death were assessed by ELISA and LDH cytotoxicity assay kit (Roche, Mannheim, Germany), respectively. When indicated,

the cells were pre-treated with 40μM of necrostatin-1 (SIGMA) 30minutes prior the stimulation to block the z-IETD+LPS-induced necroptotic cell death. Graphs show the mean ± SEM of 3 independent experiments (n=4 amount 3).

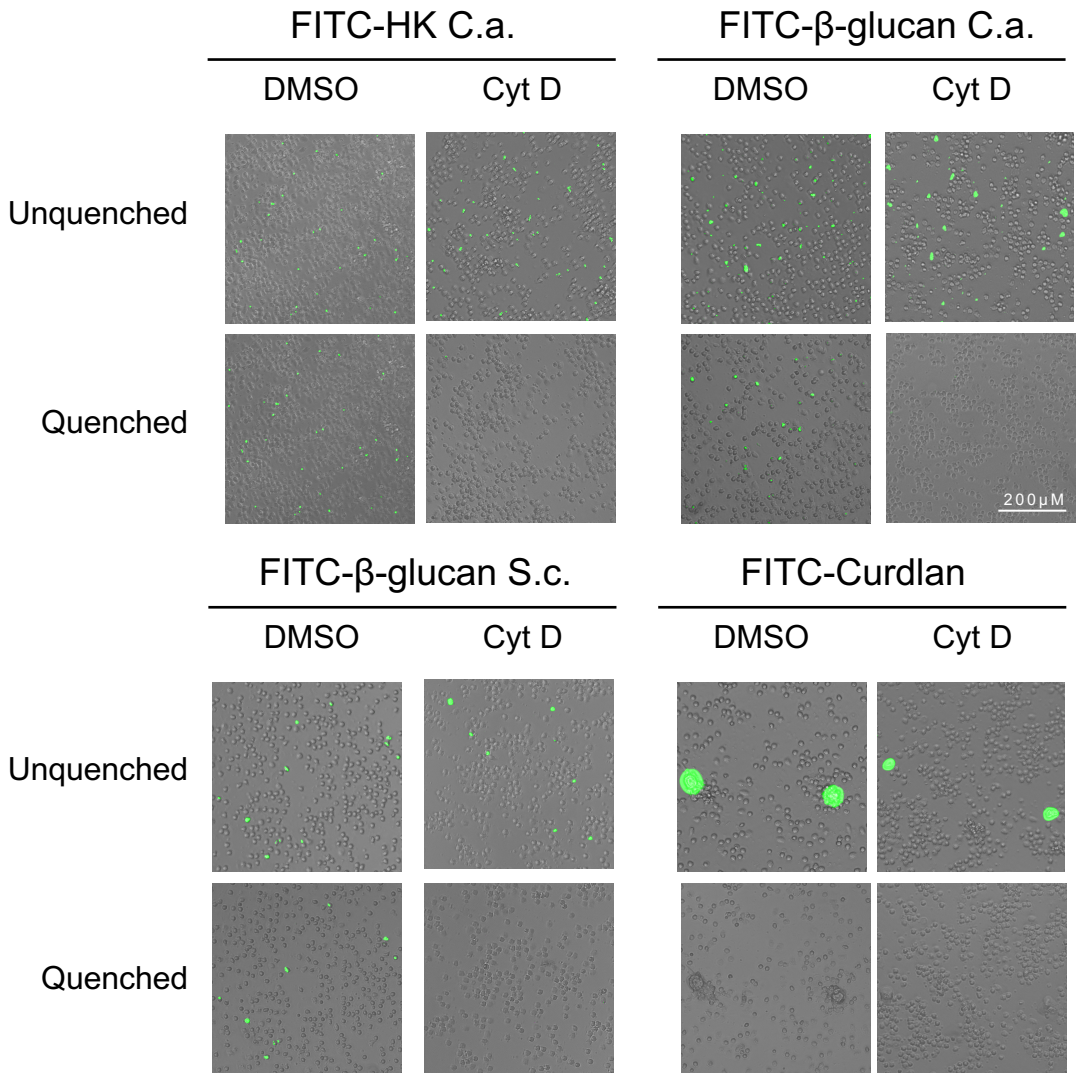

Supplementary Figure 1

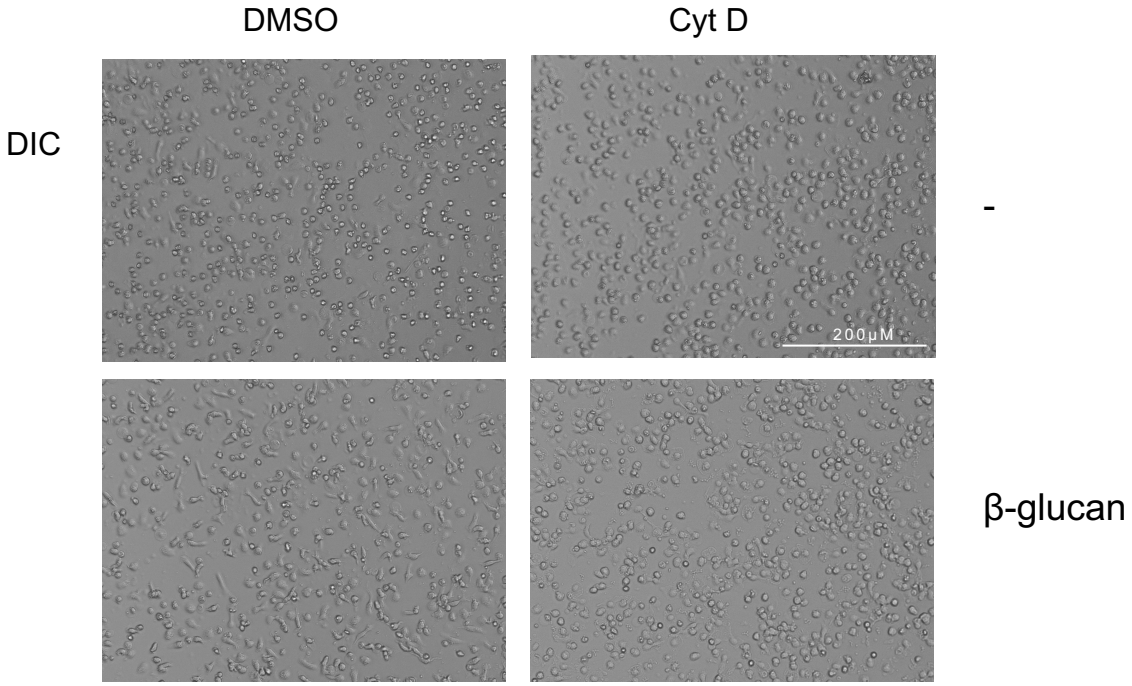

Supplementary Figure 2

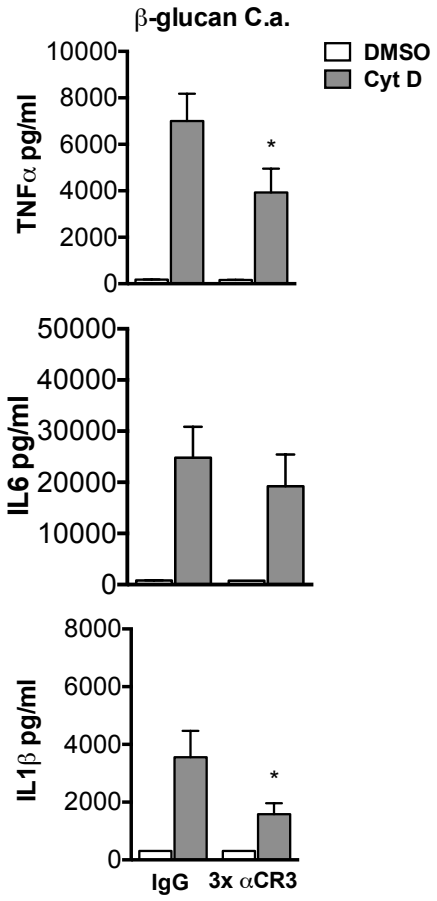

Supplementary Figure 3

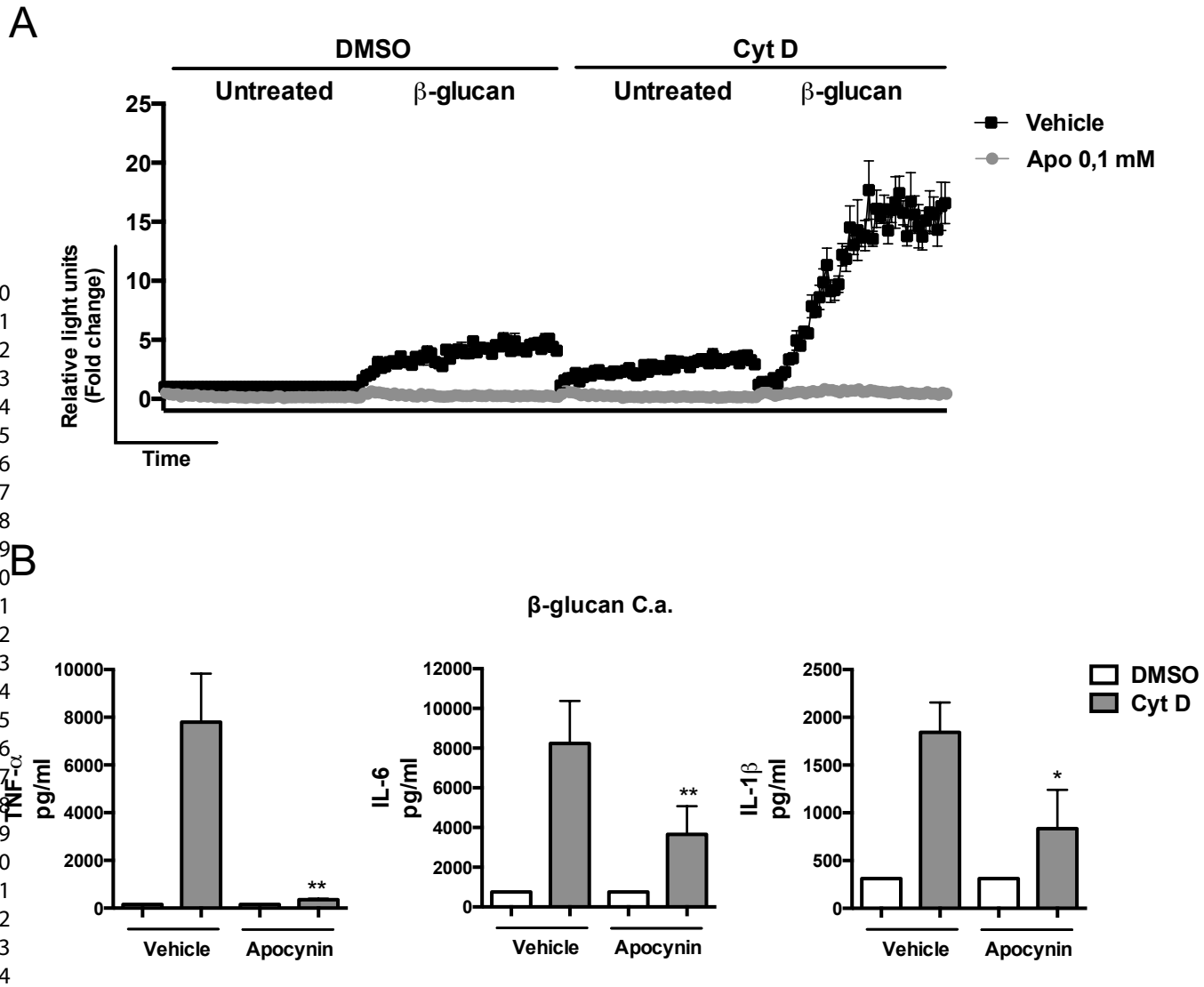

Supplementary Figure 4

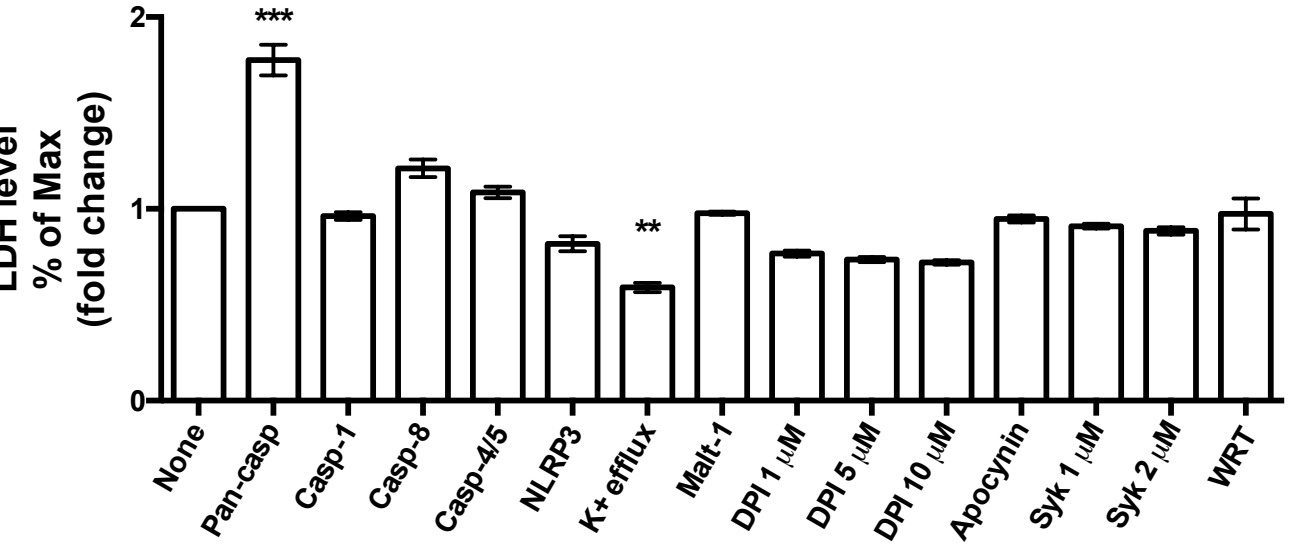

Supplementary Figure 5

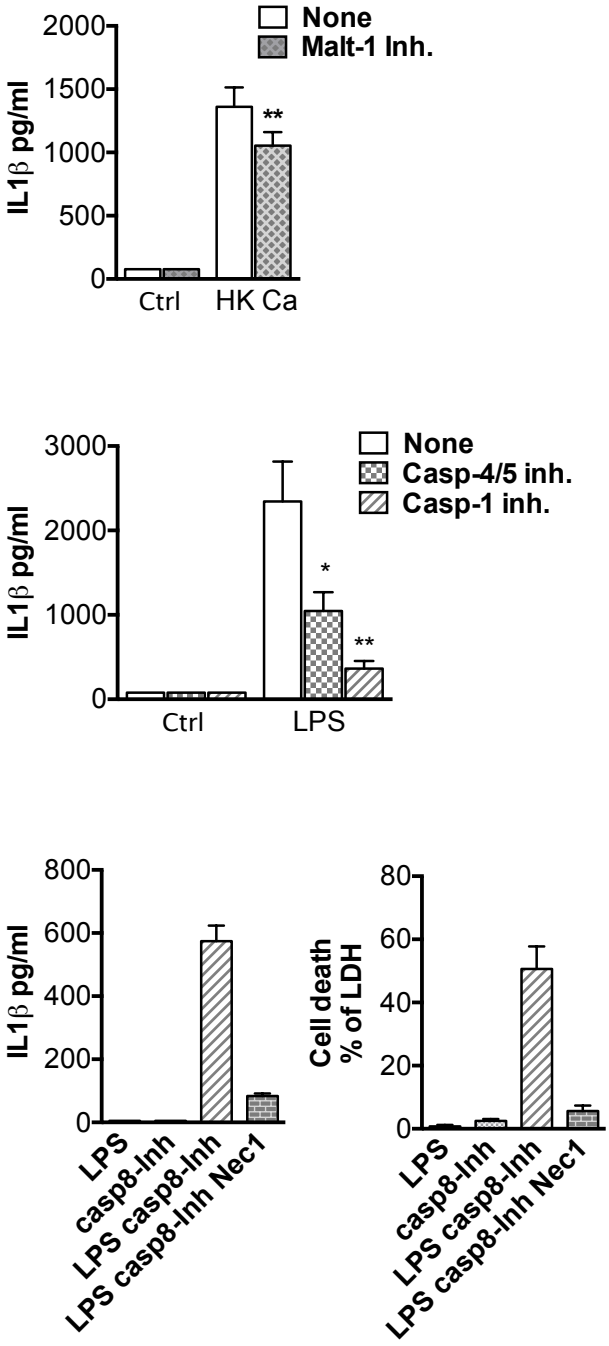

Supplementary Figure 6